Journal of Water Process Engineering 83 (2026) 109709

Contents lists available at ScienceDirect

Journal of Water Process Engineering

journal homepage: www.elsevier.com/locate/jwpe

Impact of different hydrodynamic flow regimes on antibiotic removal in anaerobic fixed-bed bioreactors: operational, ecotoxicological and microbiological aspects

Mateus Cottorello-Fonsêca [a,*], Gleyson B. Castro [b], Elias G.F. Rezende [c], Isabel K. Sakamoto [a], Francisco R.S. Freitas [a,d], Rodrigo B. Carneiro [a,e], Carolina A. Sabatini [a], Rogers Ribeiro [c], Juliano J. Corbi [b], Marcelo Zaiat [a]

[a] Laboratory of Biological Processes, Department of Hydraulic and Sanitation, São Carlos School of Engineering, University of São Paulo, 1100 João Dagnone Ave., 13563-120, São Carlos, São Paulo, Brazil
[b] Laboratory of Ecotoxicology and Applied Ecology, Department of Hydraulic and Sanitation, São Carlos School of Engineering, University of São Paulo, 1100 João Dagnone Ave., 13563-120, São Carlos, São Paulo, Brazil
[c] Environmental Biotechnology Laboratory, Department of Food Engineering, School of Animal Science and Food Engineering, University of São Paulo, 225 Duque de Caxias Norte, 13635-900, Pirassununga, São Paulo, Brazil
[d] Department of Chemistry and Environment, Federal Institute of Education, Science and Technology of Ceará (IFCE), Maracanaú Campus, 61939-140, Maracanaú, Ceará, Brazil
[e] Laboratory of Chromatography, Institute of Chemistry of São Carlos, University of São Paulo, 400, Trabalhador São-Carlense Ave., 13566-590, São Carlos, São Paulo, Brazil

ARTICLE INFO

Editor: Jing Zhang

Keywords:
Anaerobic bioreactors
Flow regimes
Antibiotics
Ecotoxicity
Microbial community

ABSTRACT

Literature has reported antibiotic overuse and the spread of antibiotic-resistant bacteria, which require better wastewater treatment. The influence of reactor hydrodynamics on antibiotic elimination processes and related environmental hazards is yet inadequately comprehended. This study assessed the impact of different flow regimes— plug-flow (PF) and continuous-stirred (CS)—on the elimination of 12 antibiotics (five fluoroquinolones, six sulfonamides, and trimethoprim; 10.0 μg L^{-1} each) in anaerobic fixed-bed bioreactors (AnFBR). Analysis of residence time distribution indicated that the PF-AnFBR functioned under almost ideal conditions (Peclet number > 1000; dead volume < 2.5%), but the CS-AnFBR had significant non-idealities, characterized by substantial dead zones (54–72%) and hydraulic short-circuiting. Despite both systems attaining elevated COD removal rates (>94%), the patterns of antibiotic removal varied considerably. Plug-flow settings promoted biodegradation-dominated elimination of sulfonamides and trimethoprim (47–100%), while the continuous-stirred arrangement improved the removal of strongly sorbing fluoroquinolones, primarily through adsorption mechanisms. Ecotoxicity assays showed reduced toxicity to *Chironomus sancticaroli* after treatment, but increased toxicity was observed for *Allonais inaequalis* and *Ceriodaphnia silvestrii*, suggesting the formation of toxic transformation products. The microbial analysis revealed a diverse population in both bioreactors, with key genera such as *Aeromonas*, *Pseudomonas*, and *Methanothrix* cleaving aromatic compounds, playing significant roles in antibiotic biodegradation, and stability in the performance of anaerobic bioreactors. These findings indicate that the hydrodynamic regime is a crucial design component influencing antibiotic behavior and environmental efficiency in anaerobic wastewater treatment.

1. Introduction

The global annual use of antibiotics has surpassed 100,000–200,000 tons [1]. Fluoroquinolones exert antimicrobial effects by inhibiting enzymes involved in DNA replication [2], but approximately 70% remain unmetabolized after administration and are released into the environment through excreta [3]. Sulfonamides are applied in the treatment of gram-positive and gram-negative bacteria [4], and

* Corresponding author at: 1100 João Dagnone Ave., 13563-120, São Carlos, São Paulo, Brazil.
E-mail address: mateus.cottorello@usp.br (M. Cottorello-Fonsêca).

https://doi.org/10.1016/j.jwpe.2026.109709
Received 24 November 2025; Received in revised form 30 January 2026; Accepted 9 February 2026
Available online 11 February 2026

sulfamethoxazole is one of the most frequently detected contaminants in wastewater [5]. Diaminopyrimidines function similarly to sulfonamides by inhibiting bacterial DNA synthesis. Trimethoprim (TMP), the first diaminopyrimidine developed, is applied in combination with sulfamethoxazole (SMX) in a 5:1 ratio (SMX:TMP) since 1968 due to its synergistic bactericidal properties [6]. The "Comprehensive Antibiotic Resistance Database" documented the emergence of 30 unique TMP resistance genes in aquatic environments [7]. Previous studies have indicated that environmentally relevant concentrations (ng to μg L^{-1}) of those classes have caused toxic effects in freshwater species [8].

Anaerobic biodegradation has proven to be an efficient mechanism for micropollutant removal (from ng to μg L^{-1}) in urban wastewater, as microorganisms can remove excess organic carbon, nitrogen, and phosphorus [9]. Anaerobic bioreactors have been used for decades worldwide, showing great applicability for the treatment of different effluents, such as sanitary sewage and wastewater from slaughterhouses and the food and dairy industries [10].

The diverse configurations of anaerobic bioreactors emphasize the importance of those designed to retain biomass on support materials, known as anaerobic fixed-bed bioreactors (AnFBR). Support material facilitates the formation of a microbial biofilm, where pollutant removal is achieved via biodegradation and biosorption [11]. The primary benefit of AnFBR is the facilitation of high cell retention times, which enables elevated microbial concentrations alongside low hydraulic retention times (HRT) [12], which helps develop slow-growing microorganisms, resulting in a diverse microbial community [13]. Moreover, the mass transfer by convection and diffusion in AnFBR is influenced by the hydrodynamic conditions of the surrounding fluid, including the fluid velocity, the particle diameter, and the physical properties of the fluid. The mass transfer coefficient through the fluid layer is directly proportional to the applied HRT and the increase in the Reynolds number of the system [11].

AnFBR are categorized into anaerobic bioreactors featuring structured fixed-bed (AnSTBR) and those with packed fixed-bed (AnPBR) [13]. Mockaitis et al. [14] are considered pioneers in using AnSTBR, employing polyurethane foams as support for biomass and evaluating cadmium toxicity in the anaerobic biodegradation of lab-made wastewater. Cunha et al. [15] employed AnSTBR and polyurethane foams for treating lab-made mine acid drainage. Carneiro et al. [16] compared the performances of AnSTBR and AnPBR using polyurethane foams in the removal of ciprofloxacin and sulfamethoxazole in lab-made wastewater.

AnFBR demonstrate versatility and capability, making them suitable for evaluating the removal performance of fluoroquinolones, sulfonamides, and diaminopyrimidines antibiotics in wastewater. Assessing flow patterns is essential for establishing the impact of flow variations on the behavior of the microbial community and, consequently, on the biodegradation of antibiotics. However, a critical and often overlooked aspect in optimizing AnFBR for antibiotic removal is hydrodynamics. The impact of different flow (e.g., plug-flow vs. continuous-stirred), as well as deviations from hydrodynamic idealities, on antibiotic removal efficiency, the microbial community, and the resulting ecotoxicity of treated effluents remains insufficiently explored.

Despite numerous studies indicating that antibiotics at environmentally relevant concentrations (ng – μg L^{-1}) do not substantially hinder organic matter removal in anaerobic bioreactors and can be partially eliminated via adsorption and biodegradation, most research implicitly presumes ideal or equivalent hydraulic behavior of bioreactors. Thus, the impact of hydrodynamic conditions on antibiotic behavior, elimination processes, microbial selection, and ecotoxicological risk is inadequately understood. The impact of departures from hydraulic ideality—such as dead zones, axial dispersion, and short-circuiting—on antibiotic–biomass interactions has been inadequately explored. Addressing this disparity is essential, since anaerobic bioreactors with comparable organic matter removal efficiencies may demonstrate fundamentally distinct performances in antibiotic attenuation and environmental safety. This study aimed to enhance existing information by directly connecting reactor hydrodynamics to antibiotic removal mechanisms, microbial activity, and post-treatment ecotoxicity in anaerobic fixed-bed bioreactors functioning under varying flow regimes.

2. Materials and methods

2.1. Target antibiotics

The 12 target antibiotics investigated were ciprofloxacin (CIP), enrofloxacin (ENR), norfloxacin (NOR), ofloxacin (OFL), pefloxacin (PEF), sulfacetamide (SCT), sulfadiazine (SDZ), sulfadimethoxine (SDX), sulfamerazine (SMR), sulfamethazine (SMZ), sulfamethoxazole (SMX), and trimethoprim (TMP), all of them purchased with high purity percentages (> 98%) from Sigma-Aldrich (*St.* Louis, MO, USA).

2.2. Operational conditions

2.2.1. Lab-made wastewater and anaerobic sludge

Lab-made wastewater with a chemical oxygen demand (COD) of approximately 600 mg L^{-1} was generated (Table S1). Anaerobic sludge sourced from an upflow anaerobic sludge blanket (UASB) reactor processing poultry slaughterhouse wastewater, characterized by total volatile solids of 25.07 ± 1.85 gTVS L^{-1}, served as the inoculum.

2.2.2. Configuration and operating conditions of anaerobic fixed-bed bioreactors

The treatment system consisted of two bench-scale acrylic reactor configurations: a PF-AnFBR and a CS-AnFBR, both using polyurethane foam (92% porosity, 23 g L^{-1} apparent density, and 43.8 m^2 g^{-1} specific surface area [17] as a support medium for anaerobic biomass immobilization (Fig. S1). PF-AnFBR (2.20 L) used vertical polyurethane foam strips (84.8% bed porosity; 15.9 g foam). CS-AnFBR (1.90 L) used 1 cm foam cubes (58% porosity; 7.4 g foam).

Prior to the start-up of PF-AnFBR and CS-AnFBR operations, the support media were inoculated with granular anaerobic sludge. The support media were inoculated with granular anaerobic sludge following the methodology by Zaiat et al. [18]. The bioreactors' operation lasted 145 days and was divided into phases according to three distinct flows, namely, Phase 1 (49 days, 122 ± 4.24 mL h^{-1}), Phase 2 (45 days, 162.5 ± 6.36 mL h^{-1}), and Phase 3 (51 days, 244 ± 8.49 mL h^{-1}), respectively.

2.3. Experimental methods

2.3.1. Residence time distribution assessment

To determine the reactor flow patterns, hydrodynamic tests were conducted using an NaCl solution (10.0 g L^{-1}) as a tracer, introduced as a step input. The concentration of dissolved particles in the effluent was continuously monitored with the use of a conductivity sensor that was attached to a data-gathering system called Vernier CON-BTA and the software Logger Lite 1.6.1 (Vernier Software & Technology) was utilized to collect data, and the results were analyzed in accordance with Levenspiel [19].

The residence time distribution (RTD) analysis was performed varying the nominal hydraulic retention time (HRT_n) of the bioreactors. For the CS-AnFBR, HRT_n of 9.26 h (122 ± 4.24 mL h^{-1}), 6.95 h (162.5 ± 6.36 mL h^{-1}) and 4.63 h (244 ± 8.49 mL h^{-1}) were assessed, corresponding to Phases 1, 2, and 3, respectively. For the PF-AnFBR, HRT_n of 15.0 h (122 ± 4.24 mL h^{-1}), 11.22 h (162.5 ± 6.36 mL h^{-1}) and 7.48 h (244 ± 8.49 mL h^{-1}) were evaluated, corresponding to Phases 1, 2, and 3, respectively. Data analysis included the construction of the normalized curve F(t), according to Eq. 1. The RTD curve E(t) was obtained by differentiation of Eq. 1, according to Eq. 2. The real HRT (t_m) of the bioreactors was calculated according to Eq. 3. The dimensionless time

(θ) (Eq. 4) and the dimensionless RTD curve E(θ) (Eq. 5) were calculated.

$$F(t) = \frac{C(t)}{C_{max}} \quad (1)$$

$$E(t) = \frac{dF(t)}{dt} \quad (2)$$

$$t_m = \int_0^{\infty} t \bullet E(t)dt \quad (3)$$

$$\theta = \frac{t}{t_m} \quad (4)$$

$$E(\theta) = t_m \bullet E(t) \quad (5)$$

where C(t) represents the tracer concentration at time t, and C_{max} denotes the maximum tracer concentration (mg L^{-1}).

The E(θ) curves, obtained for the CS-AnFBR and PF-AnFBR were fitted to the tanks in series (TIS) (Eq. 6) and axial dispersion (AxD) (Eq. 7) models, respectively. Calibration was performed with the aim of estimating the number of tanks (N) and the Peclet (*Pe*) number, for the TIS and AxD models, respectively. The volume of dead zones (V_d) was calculated based on the value of t_m obtained in the hydrodynamic assays and HRT_n applied in the bioreactors, according to Eq. 8 [20]. The presence of hydraulic short-circuiting (Z_c) was assessed by the relation of the time of first appearance of tracer in the effluent (peak) and the t_m, applying Eq. 9 [21].

$$E(\theta) = N\frac{(N\theta)^{N-1}}{(N-1)!}e^{-N\theta} \quad (6)$$

$$E(\theta) = \frac{1}{\sqrt{(4 \bullet \pi)/Pe}}\exp\left[-\frac{(1-\theta)^2}{4/Pe}\right] \quad (7)$$

$$V_d = V_w \bullet \left(1 - \frac{t_m}{HRT_n}\right) \quad (8)$$

$$Z_c = \frac{t_p}{t_m} \quad (9)$$

where V_w is the working volume (L), HRT_n is the nominal HRT applied in the reactor (h), and t_p is the time of peak of the E(t) curve.

The quality of the fitting between the experimental data and the TIS e AxD models was evaluated with the normalized root mean squared error (NRMSE, Eq. 10).

$$NRMSE = \frac{\sqrt{\frac{1}{m \bullet n}\sum_{k=1}^{m}\sum_{i=1}^{n}\left(C_{exp}(t_i) - C_{sim}(t_i, \rho)\right)^2}}{C_{max} - C_{min}} \bullet 100 \quad (10)$$

where m is the number of variables measured (in this case, m = 1), n is the number of experimental data points, C_{exp} and C_{sim} are the experimental and simulated values of tracer concentration, ρ is the calibrated parameter and C_{max} and C_{min} are maximum and minimum values of experimental tracer concentration.

2.3.2. Analytical chemistry

The system performance was assessed through physicochemical analyses of influent and effluent samples from the bioreactors, according to the methodologies outlined in APHA [22] - pH (4500-H+ B), COD (5220-D), and suspended solids (2540-E). Alkalinity was quantified by the titration method of Ripley et al. [23] and volatile fatty acids were assessed via gas chromatography with a flame ionization detector (GC-FID) following the Adorno et al. [24] methodology. All the tests were conducted on triplicate.

The concentrations of the 12 antibiotics were quantified through a column-switching online solid-phase extraction integrated with liquid chromatography/tandem mass spectrometry (SPE-LC-MS/MS: Agilent 1200 LC series and AB SCIEX QTRAP 5500), in accordance with the methodology developed by Lima Gomes et al. [25]. The calibration curves for the antibiotics were built on the antibiotic-free matrix for ensuring accuracy and precision. Three transitions were examined for each analyte, and the most significant fragment was selected for measurement—the remaining ones served a confirming function. The detection limits and transitions monitored for each antibiotic are detailed in Table S2. Every test was carried out in triplicate.

2.3.3. Acute ecotoxicity analysis

Allonais inaequalis, *Ceriodaphnia silvestrii*, and *Chironomus sancticaroli* species were cultured according to Castro et al. [26], ABNT [27], and Corbi et al. [28] methodologies, respectively (Section 3, Supporting Information). The species were chosen based on their representation of unique ecological functions in the aquatic ecosystem. Wastewater samples were collected from the bioreactors and diluted at proportions of 1%, 6%, 12%, 25%, and 50% as a water medium of exposure, which represents natural dilution scenarios during discharge [29]. The 100% treatment was undiluted and represented the raw sample.

For *A. inaequalis* assays, Corbi et al. [30] and Castro et al. [26] methodologies were used. Each replicate (triplicate) had six 4–6 mm individuals randomly distributed throughout the treatments. Each replicate containing 240 mL of water medium and 60 g of autoclaved fine sand. *A. inaequalis* species were fed with 2 mg of macerated TetraMin® per replicate. Similarly, triplicate controls contained six individuals, 240 mL culture water, 60 g autoclaved fine sand, and 2 mg macerated TetraMin®. Assays were maintained at 25 ± 1 °C with a 12 h light/12 h dark photoperiod. After 96 h, mortality rates were obtained by counting survivors.

The C. silvestrii assays followed ABNT [27]. Five neonates under 24 h old were randomly distributed among the treatments per replicate (triplicate) containing 30 mL water medium. Controls (triplicate) contain five neonates per replicate and 30 mL culture water. The assays were kept at 27 °C and for a 12 h light/12 h dark photoperiod. After 48 h, immobility rates were determined by counting the mobile individuals.

The *C. sancticaroli* assays were followed Fonseca [31] and OECD [32] methods. Six larvae of III–IV instars were randomly distributed among the treatments (triplicate), containing 240 mL of water medium and 60 g of autoclaved fine sand and fed with 2.5 mg of macerated TetraMin® per replicate. Controls (triplicate) contain six individuals, 240 mL culture water, 60 g autoclaved fine sand, and 2.5 mg macerated TetraMin®. The assays were maintained at 25 ± 1 °C and for a 12 h light/12 h dark photoperiod. After 96 h of exposure, mortality rates were determined by recording the living individuals. All toxicity assays were performed twice.

2.3.4. Statistical analysis

A Shapiro-Wilk test was applied to verify the samples normality. Subsequently, a *t*-test was performed to evaluate the COD and 12 antibiotics removal efficiencies in PF-AnFBR and CS-AnFBR operation, which the bioreactors' performance was considered statistically different when $p < 0.05$. In addition, a one-factor ANOVA test (Welch) analyzed the differences in the HRT_n applied to average COD and antibiotics removal. The significant difference in this HRT_n was indicated by $p < 0.05$. These statistical analyses were conducted using JAMOVI 2.3.28 software.

Regarding the acute ecotoxicity analysis, significant differences in mortality or immobility rates of *species* between treatments and controls were investigated using the Kruskal-Wallis test, followed by a multiple comparison test of *p*-values, after checking the data normality by Shapiro-Wilk test. The lethal concentrations of the samples on 50% (LC50 or EC50) of the exposed individuals were obtained from R 3.5.0 software, and the reduction or increase in toxicity was estimated from the difference between effluent and influent. The statistical treatment was performed in Statistica 10.0 software.

2.4. Microbial community analysis

2.4.1. DNA extraction and testing

The sequencing analysis was performed at the end of the PF-AnFBR and CS-AnFBR to guarantee representative microbiological characterization. Biomass samples adhered to the fixed-bed bioreactors were repeatedly rinsed with distilled water and subsequently sieved to eliminate the support material. The "Qiagen DNeasy PowerSoil Pro Kit" from Thermo Fischer (Hilden, Germany) was used for the genomic DNA extraction. The "DNeasy PowerSoil Pro Kit Handbook" manufacturer's protocol was followed using the solutions provided by the kit and the instructions for extraction. The DNA concentration in ng μL^{-1} was subsequently determined by aliquoting each sample (2.0 μL) and quantifying it using a Thermo Scientific NanoDrop 2000 spectrophotometer. All samples exceeded the minimum recommended level of 30.0 ng μL^{-1} [33]. Afterwards, samples were stored at −20 °C until analysis. The method was previously described by Cottorello-Fonsêca et al. [34].

2.4.2. Amplicon sequencing and bioinformatics analysis

The genomic DNA samples from the bioreactors were sent to ByMyCell laboratory (Ribeirão Preto/SP, Brazil), where massive sequencing of the 16S rRNA gene in V3-V4 regions of the gene was performed on an Illumina PE250 platform and a basic bioinformatics analysis was conducted for taxonomy and metabolism prediction The DNA samples were prepared for amplicon library amplification, then the marker gene was amplified with 341F/806R [35] and 515F/806R [36]. The sequences were processed on the Qiime2 Platform and the readings were mapped against the reference 16S rRNA database (Silva 138 99% ASV full length of sequences). The functional potential of the microbial community was analyzed using PICRUSt2 (Phylogenetic Investigation of Communities by Reconstruction of Unobserved States), with the results predicted using the Kyoto Encyclopedia of Genes and Genomes (KEGG) database for the prediction of metabolic pathways. The complete sequencing dataset supporting these findings has been deposited in the NCBI Sequence Read Archive under BioProject reference number PRJNA1229479 (samples SAMN47130392 to SAMN47130395) (Section 6, Supporting Information).

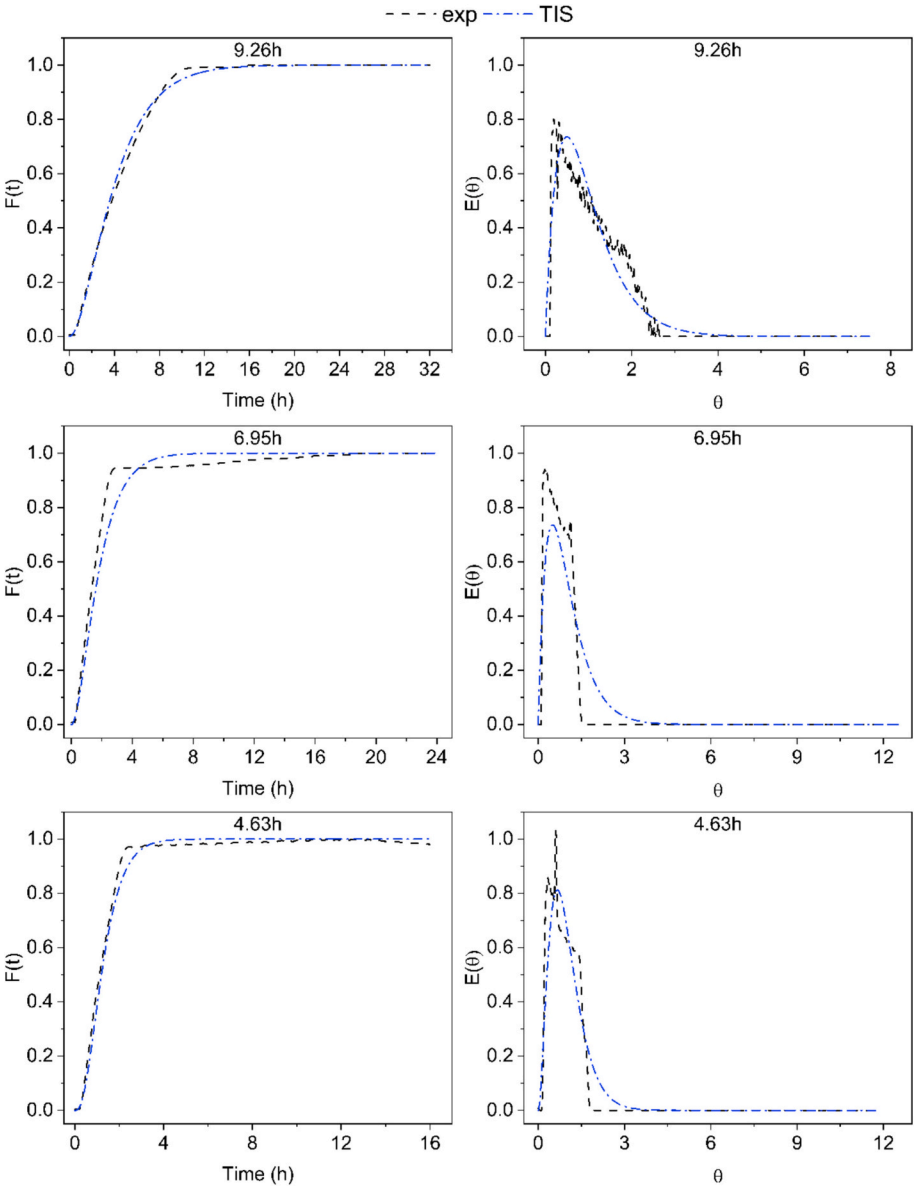

Fig. 1. Normalized curve F and exit age curve E(θ) for the CS-AnFBR, including experimental measurements (black dashed line) and simulated data using the TIS model (blue dashed line). (For interpretation of the references to colour in this figure legend, the reader is referred to the web version of this article.)

3. Results and discussion

3.1. Reactor hydrodynamics

The F(t) and E(θ) for the CS-AnFBR revealed distinct hydrodynamic patterns depending on the operating condition (Fig. 1). Table 1 summarizes the main hydrodynamic parameters obtained in the calibration of the CS-AnFBR. In all cases, the TIS model was able to adequately reproduce the experimental curves, with NRMSE ranging between 6.0 and 8.7%.

At 9.26 h HRT_n, the system exhibited behavior consistent with two ideal bioreactors in series (N ≈ 2). The E(θ) curve presented a moderate dispersion around the mean residence time, with a relatively symmetric peak (t_p = 0.83 h). As the HRT_n decreased to 6.95 h, the reactor maintained N ≈ 2, but the E(θ) curve became more asymmetric, with an earlier peak (t_p = 0.43 h), indicating a higher degree of short-circuiting (Z_c = 0.23). At 4.63 h HRT_n, the model adjustment indicated $N = 3$, suggesting a higher degree of axial mixing. In this condition, E(θ) peak shifted to later times (t_p = 0.81 h), and Z_c markedly increased to 0.61. This finding indicated that under high flow rates, part of the fluid bypassed the main reactor volume, leading to a less uniform RTD.

The analysis of V_d and Z_c offered more information about the non-idealities of the CS-AnFBR. The estimated V_d ranged from 0.59 to 0.80 L, representing approximately 54–72% of the total reactor capacity. Such values were high compared to the theoretical expectation of negligible stagnant zones in well-mixed systems. The presence of these regions could be attributed to the internal configuration of the fixed-bed reactor, where flow channeling around the packing material and localized areas with limited fluid exchange may occur. These stagnant zones reduced the effective working volume, leading to discrepancies between HRT_n and t_m [37].

Short-circuiting effects were also evident, with the index increasing markedly from 0.20 at 9.26 h to 0.61 at 4.63 h. This progressive increase indicated that, under shorter HRT_n, a significant fraction of the influent bypassed the bulk liquid phase, reaching the outlet with minimal contact time. Such behavior was consistent with the sharper, earlier peaks observed in the E(θ) curves at intermediate HRT_n and the shift toward more asymmetric RTD profiles. Short-circuiting undermines the homogeneity of the flow and reduces the efficiency of substrate-biomass interaction, as part of the influent could not be effectively treated within the reactor volume [38].

The combined influence of dead zones and short-circuiting highlighted the sensitivity of the CS-AnFBR hydrodynamics to operational conditions. While the fixed-bed design promoted biomass retention, it simultaneously introduced structural heterogeneities that impaired ideal operation. From a process engineering standpoint, these non-idealities suggested that the reactor could exhibit reduced resilience to load fluctuations and a diminished capacity for full pollutant degradation under reduced HRT_n. Nevertheless, identifying and quantifying these deviations is essential for the development of reliable reactor configurations and for the optimization of reactor design and operation [37].

Fig. 2 shows the experimental and simulated F(t) and E(θ) curves obtained for the PF-AnFBR under different HRT_n. Table 1 summarizes the main hydrodynamic parameters obtained in the calibration of the PF-AnFBR with the AxD model. The F(t) displayed a sharp step-like behavior, and the corresponding exit age distributions E(θ) were characterized by narrow peaks centered close to the mean residence time, consistent with plug-flow behavior [19]. The AxD model provided an excellent fit to the experimental curves, with NRMSE values consistently below 6.5%.

At 15.0 h HRT_n, the system exhibited a very low dispersion coefficient (D/uL = 0.0009) and a corresponding Peclet number above 1100, indicating minimal axial mixing. The E(θ) curve in this condition was highly concentrated, with a peak at t_p = 15.4 h. Similar results were observed at intermediate (11.22 h, t_p = 11.4 h) and short (7.5 h, t_p = 7.95 h) HRT_n. In all cases, the model adjustment yielded Peclet numbers above 1000 and D/uL = 0.0009, indicating a stable hydrodynamic regime across operational conditions. The peaks of the E(θ) curves remained sharp and centered at the t_m, with only slight broadening at lower HRT_n.

The calculated V_d was practically negligible (0.0001–0.045 L, ≤ 2.38% of the total volume), which contrasted with the CS-AnFBR. Likewise, the short-circuiting index remained close to unity under all conditions (1.03–1.06), further confirming the absence of preferential flow paths or significant bypassing [39]. Together, these parameters demonstrated that the PF-AnFBR operated under highly ideal plug-flow conditions, ensuring that the entire influent stream was uniformly exposed to the biomass bed.

From a process perspective, the nearly ideal hydrodynamics of the PF-AnFBR provided a longer and more homogeneous contact time between substrate and biomass compared to the CS-AnFBR. This is particularly advantageous under reduced HRT_n, as the uniform flow reduces performance losses and enhances reactor stability. The clear contrast between the two systems highlights the role of reactor configuration in determining hydraulic efficiency and its implications for pollutant removal.

3.2. Organic matter and antibiotic removal

After assessing sample normality with the Shapiro-Wilk test, statistical analysis revealed significant differences ($p < 0.05$) in COD removal among the bioreactors. PF-AnFBR removed 96.2% COD, whereas CS-AnFBR managed 94.2%. Checking variations in the HRT_n administered concerning the average COD removal, a statistically significant difference was evident in the HRT_n used for COD removal in both bioreactors, indicated by a $p < 0.05$. Regarding the HRT_n applied, PF-AnFBR showed $p = 0.003$, whereas CS-AnFBR obtained a p-value <0.001. Moreover, the bioreactors subjected to a higher HRT_n exhibited the highest average COD removal efficiency. The efficiency of PF-AnFBR was 97.8 ± 1.85%, whereas that of CS-AnFBR was 96.5 ± 2.31% (Fig. S2).

Considering the decrease in HRT_n, a consequent decrease in COD removal efficiency in the bioreactors was expected. However, this behavior was not observed for both PF-AnFBR and CS-AnFBR (Table S3). The sustained high average COD removal efficiency in the PF-AnFBR and CS-AnFBR bioreactors results from the anaerobic microbial community's metabolic processes, which effectively convert organic matter into intermediate compounds, including volatile fatty acids, and subsequently into methane. The pH stability maintained between 7 and 8 during bioreactors operation (Tables S7 and S8) provided a conducive environment for methanogenic archaea performance.

Nachaiyasit and Stuckey [40] examined the effects of variations in influent load by isolating changes in HRT and COD within a compartmentalized anaerobic reactor, addressing the discrepancies in these effects. While an increase in COD influent could modify the kinetics of

Table 1
Hydrodinamic parameters obtained with the calibration of TIS and AxD models for the CS-AnFBR and PF-AnFBR.

CS-AnFBR						
HRT_n (h)	t_m (h)	N	V_d (L)	Z_c	t_p (h)	NRMSE (%)
9.26	4.26	2.0	0.59	0.19	0.83	7.63
6.95	1.90	2.0	0.79	0.22	0.43	8.67
4.63	1.34	3.0	0.78	0.60	0.81	6.04

PF-AnFBR						
HRT_n (h)	t_m (h)	*Pe*	V_d (L)	Z_c	t_p (h)	NRMSE (%)
15.0	14.6	1111.06	0.04	1.05	15.4	6.04
11.22	11.1	1101.01	0.02	1.03	11.4	4.69
7.48	7.48	1084.63	0.0001	1.06	7.93	6.31

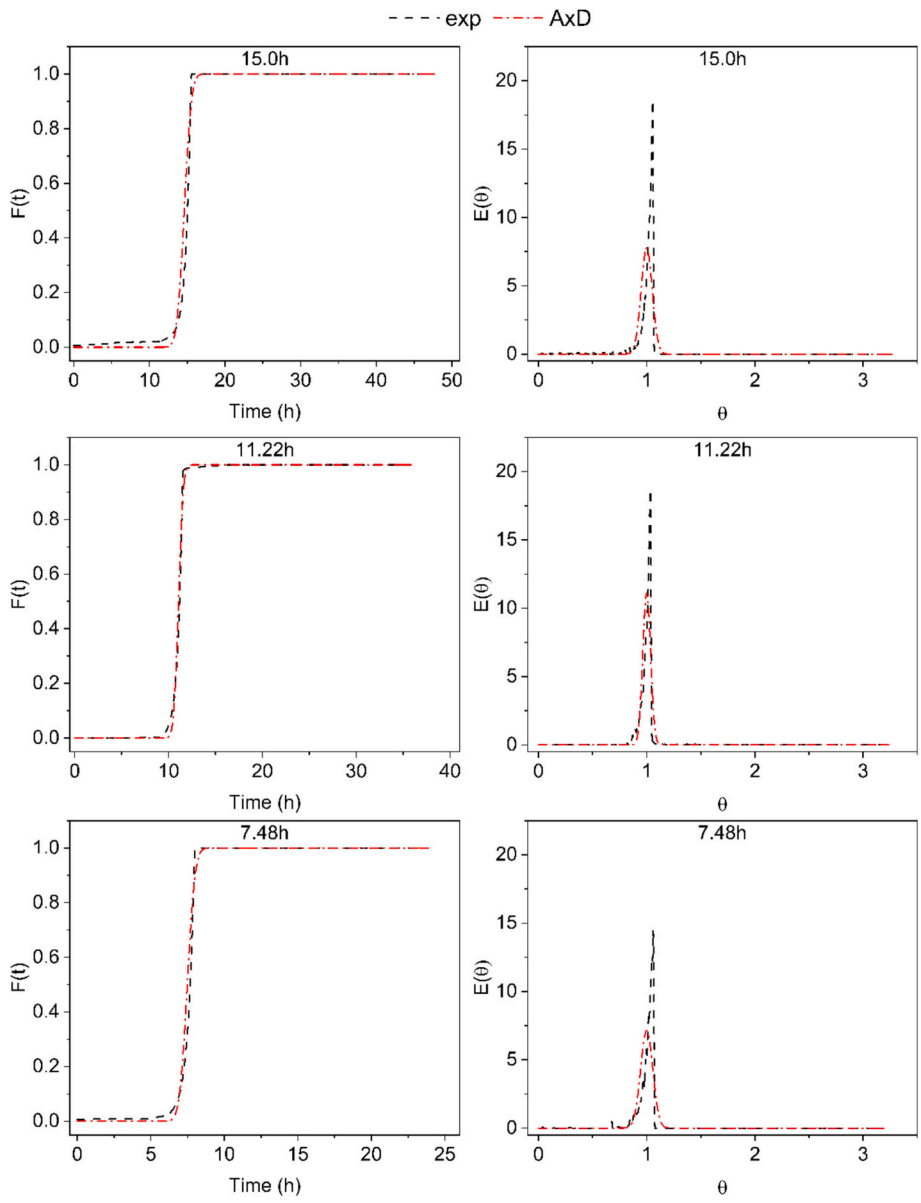

Fig. 2. Normalized curve F and exit age curve E(θ) for the PF-AnFBR, including experimental measurements (black dashed line) and simulated data using the AxD model (red dashed line). (For interpretation of the references to colour in this figure legend, the reader is referred to the web version of this article.)

biochemical reactions and intensify mass transfer processes, the authors highlighted that variations in HRT lead to hydrodynamic changes that elevate the load. This, in turn, affects the distribution of microorganisms within a biofilm, the extent of reactor mixing, and shear forces. Moreover, the alterations may influence electron transfer between species.

Different HRT in anaerobic bioreactors can modify microbial community performance, altering biomass groups selection [41]. Arcand et al. [42] noted that in a UASB reactor processing synthetic wastewater, an increase in organic loading coupled with a reduction in HRT enhances the activity of bacteria that metabolize organic acids, while simultaneously decreasing the activity of acidogenic bacteria that utilizes glucose. Carneiro et al. [12] observed that while utilizing three distinct HRTs of 12, 8, and 4 h, the average COD removal for the 12- and 8-h HRTs did not exhibit significant variation, remaining at 94.0% and 95.0%, respectively. Nevertheless, with an HRT of 4 h, the COD removal decreased to 87.5%.

Anaerobic biodegradation initiates at the biofilm–liquid interface and progresses inward through the porous support material, governed by substrate diffusion and microbial stratification within the biofilm matrix [14]. The presence of porous materials, such as polyurethane foams used in PF-AnFBR and CS-AnFBR, facilitate thin-layer diffusion by increasing the effective surface area and promotes the growth of microbial biomass and mass transfer by diffusion. Moreover, in fixed-bed bioreactors, the cell retention time is independent of HRT, which can alter the responses of the microbial community, and influence the selection of microorganism groups. CS-AnFBR contained a packed bed with a randomly distributed support material, which could lead to dead zones and bed clogging. Instead, PF-AnFBR had the bed reaction parallel to the flow stream, increasing bed porosity and minimizing preferential flow paths and clogging [14,43]. These characteristics may explain the greater effectiveness of PF-AnFBR in removing antibiotics, especially the sulfonamides and diaminopyrimidines (Fig. 3).

As shown in Table S3, the PF-AnFBR operated at the highest HRTn (15.0 h) achieved complete removal of TMP and CIP, as well as high removal of SMX (83.3 ± 13.4%) and ENR (81.3 ± 7.04%). Similarly, under the highest HRTn applied to the CS-AnFBR (9.26 h), complete removal of ENR (100 ± 0.00%) was observed, accompanied by substantial removal of SMX (79.5 ± 16.2%) and TMP (81.3 ± 8.30%). In

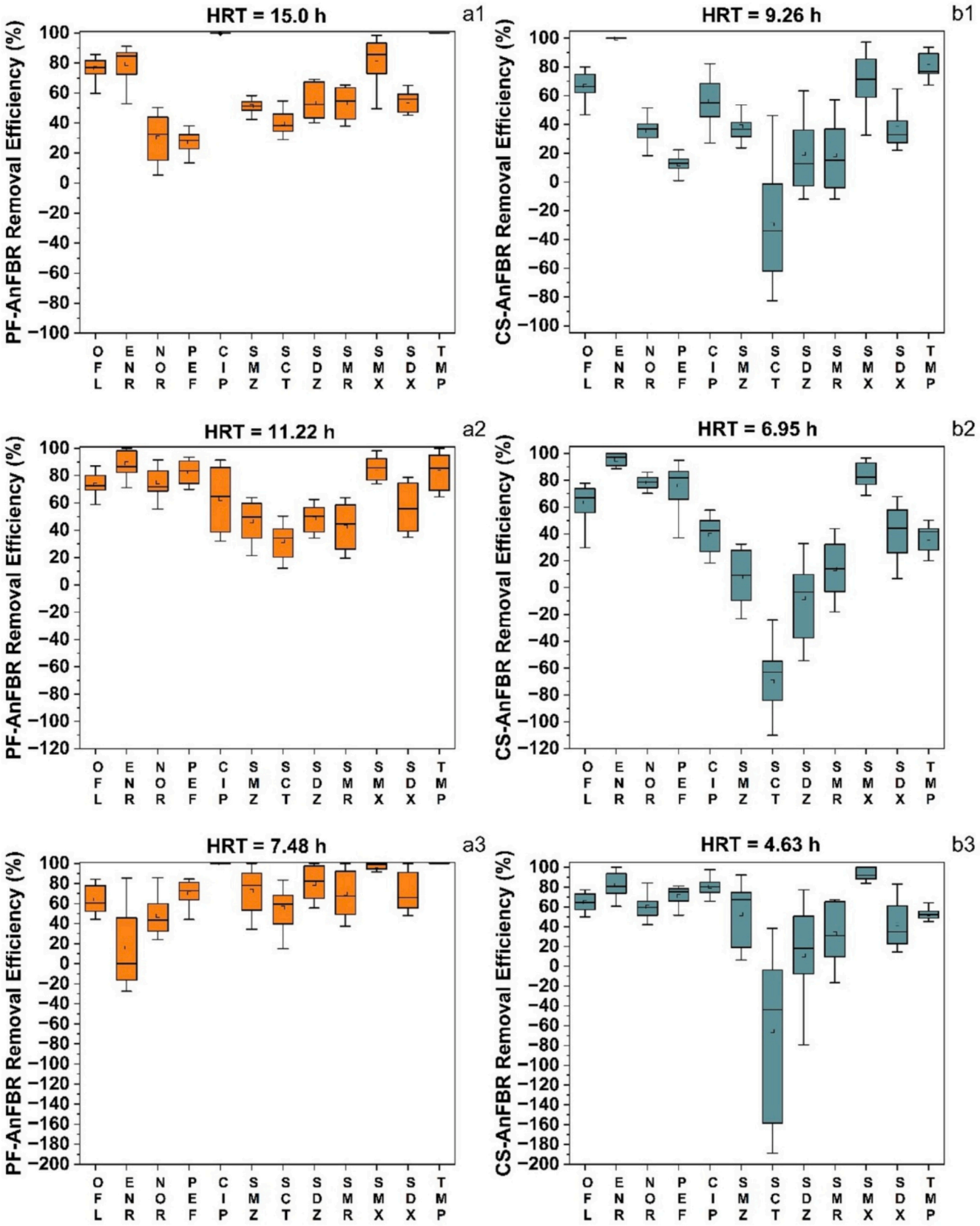

Fig. 3. Boxplot of antibiotics removal efficiency in PF-AnFBR (a1, a2, and a3) for the 15.0, 11.22 and 7.48 h HRT_n applied and CS-AnFBR (b1, b2, and b3) for the 9.26, 6.95 and 4.63 h HRT_n applied. Values described in detail in Table S3.

contrast, SCT exhibited negative removal efficiencies in the CS-AnFBR at all evaluated HRTn conditions, indicating either insufficient biodegradation or the occurrence of desorption phenomena from the reactor biofilm during operation.

A reduction of the HRT_n to 11.22 h in PF-AnFBR resulted in enhanced removal efficiencies of several antibiotics, e.g., ENR (88.9 ± 17.6%), NOR (72.9 ± 13.0%), PEF (81.7 ± 9.10%), and SMX (86.1 ± 9.03%). Likewise, the reduction of the HRT_n to 6.95 h in CS-AnFBR demonstrated improved elimination of NOR (78.3 ± 5.26%), PEF (81.7 ± 9.54%), SMR (22.3 ± 15.0%), and SMX (86.3 ± 7.78%), suggesting that moderately lower HRTn values favored the removal of selected fluoroquinolones and sulfonamides. At the minimum HRT_n (7.48 h) for PF-AnFBR, the reactor demonstrated the highest overall antibiotic removal, achieving complete elimination of CIP and TMP and significantly enhanced efficiencies for SMX (97.5 ± 3.21%), SDZ (70.0 ± 23.6%), SDX (70.2 ± 21.0%), SMR (70.1 ± 22.4%), and SMZ (68.5 ± 24.6%). In the CS-AnFBR, enhanced removal at 4.63 h was noted for CIP, SDZ, SMR, SMZ, and SMX.

Statistical analysis validated significant disparities in antibiotic elimination among the bioreactors. After assessing sample normality with the Shapiro-Wilk test, a *t*-test (95% confidence level) revealed no statistically significant difference just for OFL removal ($p = 0.175$). The PF-AnFBR exhibited markedly superior removal efficiencies for CIP, PEF, SCT, SDX, SDZ, SMR, SMX, SMZ, and TMP, while the CS-AnFBR demonstrated enhanced performance for ENR and NOR.

The impact of HRT_n on antibiotic removal was then evaluated using one-way ANOVA (Welch). In the PF-AnFBR, the removal of CIP, SCT and TMP did not exhibit significant variation between 7.48 and 15.0 h, however PEF removal was notably influenced by HRT_n, achieving maximum efficiency at 11.22 h. The removal of SDZ, SMR, SMX, and SMZ was markedly improved at 7.48 h, but the removal of SDX was not significantly affected by HRT_n. In the CS-AnFBR, statistically significant differences among HRT_n were noted, with the maximum removal efficiency for ENR at 9.26 h and NOR occurring at 6.95 h.

The hydrodynamic characteristics of the surrounding fluid, including fluid velocity, particle diameter, and physical parameters, affect mass transfer by convection and diffusion in fixed-bed bioreactors. As mentioned in item 3.1, applying the lowest value of HRT_n (4.63 h) resulted in the highest axial agitation in the CS-AnFBR. However, V_d, which was 54–72% of the reactor capacity, and Z_c, 0.20–0.61, deviated from ideality. Despite the deviations from ideality, it can be inferred that the increase in flow rates for the CS-AnFBR and the flow configuration may have facilitated an increased number of adsorption-free sites in the anaerobic biomass, since antibiotics with high adsorption potential, such as fluoroquinolones, are removable in CS-AnFBR. This study examined fluoroquinolones with carboxylic acid and a piperazinyl heterocyclic group, and furthermore, their high molecular weight indicated resistance to hydrolysis, making adsorption a feasible method for anaerobic removal [44].

Fluoroquinolones have high solid-liquid partition coefficient (K_D) and sorption rate constant of antibiotic (k_{sor}) values, indicating a high affinity for adsorption, contributing to electrostatic interactions with the microbial biofilm, cation exchange, and cationic bridging [34,45]. Cottorello-Fonsêca et al. [34] reported that fluoroquinolones (e.g., ENR, NOR, OFL, and PEF) had very high k_{sor} values (100–104 L $gTSS^{-1}$ d^{-1}) and comparatively high K_D values (0.19–0.65 L $gTSS^{-1}$), indicating a robust affinity for solid-phase adsorption. In contrast, sulfonamides (e.g., SCT, SDX, SMX, SMZ) and TMP exhibited significantly lower K_D (0.01–0.09 L $gTSS^{-1}$) and k_{sor} (27–28 L $gTSS^{-1}$ d^{-1}), indicating that adsorption is not the primary mechanism of their removal.

Based on hydrodynamic data (item 3.1), the PF-AnFBR demonstrated operational stability at all applied HRT_n, with low D/u.L (< 0.001) and *Pe* above 1000. Moreover, the deviations from ideality could be neglected, with V_d representing less than 2.5% of the total reactor volume and Z_c values close to 1.0 indicating the absence of preferential paths. Thus, the near-ideal plug-flow conditions of the PF-AnFBR, with minimum axial dispersion and no short-circuiting, extended and uniform substrates-biomass contact time and facilitated biodegradation pathways, which sulfonamides and TMP, characterized by low K_D values and weak sorption affinity, exhibited significantly higher removal in the PF-AnFBR (Table S3). Aromaticity and electronegativity affect sulfonamide adsorption and ionization, while pyrimidine, dimethylpyrimidine, and dimethoxypyrimidine increase the Freundlich constant (k_F), affecting adsorption [46].

Since SCT and SMX lack aniline, their removal differed. The initial reaction generates nitroso and nitro-substituted sulfonamide by transferring electrons between SO_4^- and the aromatic amine [34]. Sulfonamide bioactivity can be lost by amine oxidation. When reactive oxygen species are abundant, the nitro-substituted sulfonamide S—C bond breaks. The intermediates break down into mineral acids, inorganic anions, CO_2, and H_2O when the ring opens [47]. Both aniline and pyrimidine and one acidic group make up sulfonamides SDX, SDZ, SMR, and SMZ. SO_4^- hits the electron donor aniline first, and hydrogen transfer in the sulfonamide starts cleavage after electron transfer. Biodegradation produces sulfanilic acid and 4-amino-2,6-dimethoxypyrimidine after cleavage, and SMX and SCT, which lack aniline, deteriorate slower [48].

In Fig. 3, only SCT was not removed efficiently in CS-AnFBR. PF-AnFBR achieved above 30.0% SCT removal efficiency. Oliveira et al. [41] treated swine wastewater utilizing the horizontal anaerobic reactor with immobilized biomass (HAIB) and a 24 h HRT for removing organic matter and SMZ. The authors attributed negative SMZ removal efficiency ratings to the release of antibiotics from the sludge. Therefore, the negative removal efficiencies observed for SCT in the CS-AnFBR could be attributed to the release of previously adsorbed antibiotics from the biomass or support material, a phenomenon exacerbated by the hydrodynamic irregularities (e.g., channeling and dead zones) in this reactor configuration. In contrast, the stable plug-flow conditions of the PF-AnFBR likely prevented such release, resulting in positive removal.

The differing behaviors noted among bioreactors functioning under various hydrodynamic regimes (Table S3) indicate that reactor hydraulics had a more significant impact on antibiotic destiny than interactions between antibiotics. The CS-AnFBR facilitated the exposure of new adsorption sites, advantageous for fluoroquinolones, while the PF-AnFBR encouraged a uniform residence time distribution and prolonged biofilm interaction, hence improving co-metabolic biodegradation of low-K_D compounds. This suggests that biodegradation, rather than adsorption, controlled sulfonamides and TMP elimination, and that fluoroquinolones did not significantly impede these processes.

3.3. Acute ecotoxicity assessment

Fig. 4 illustrates the mortality (*A. inaequalis* and *C. sancticaroli*) and immobility (*C. silvestrii*) rates after PF-AnFBR and CS-AnFBR influent and effluents exposures. The PF-AnFBR ($HRT_n = 11.22$ h) and CS-AnFBR ($HRT_n = 4.63$ h) effluents exhibited the lowest toxicity values for *A. inaequalis*, recorded at −5.30 and − 0.08, respectively, when assessing 50% of the individuals exposed to the influent and effluent of the bioreactors across the three HRT_n (Table S4). Exposure to PF-AnFBR and CS-AnFBR effluents under all HRT_n increased *C. silvestrii* immobility. Concerning *C. sancticaroli*, the quantification of lethality was not feasible; however, as shown in Fig. 4, the species showed the lowest mortality rates when subjected to effluents from the bioreactors compared to *A. inaequalis* and *C. silvestrii*.

The mortality rate of *A. inaequalis* exposed to reactor influent samples ranged from 4.4 ± 7.7% at 1% influent to 16.6 ± 12.6% at 100% influent (Fig. 4a). Additionally, studies using 100% effluents from PF-AnFBR and CS-AnFBR resulted in the highest mortality rates across all the HRT_n assessed. Significant variations in *A. inaequalis* mortality rates were found between 100% influent and 100% effluent treatments, with the highest HRT_n for both bioreactors ($H = 57.32$; $p < 0.05$, Kruskal-Wallis test). Significant differences ($p < 0.05$) were observed in the

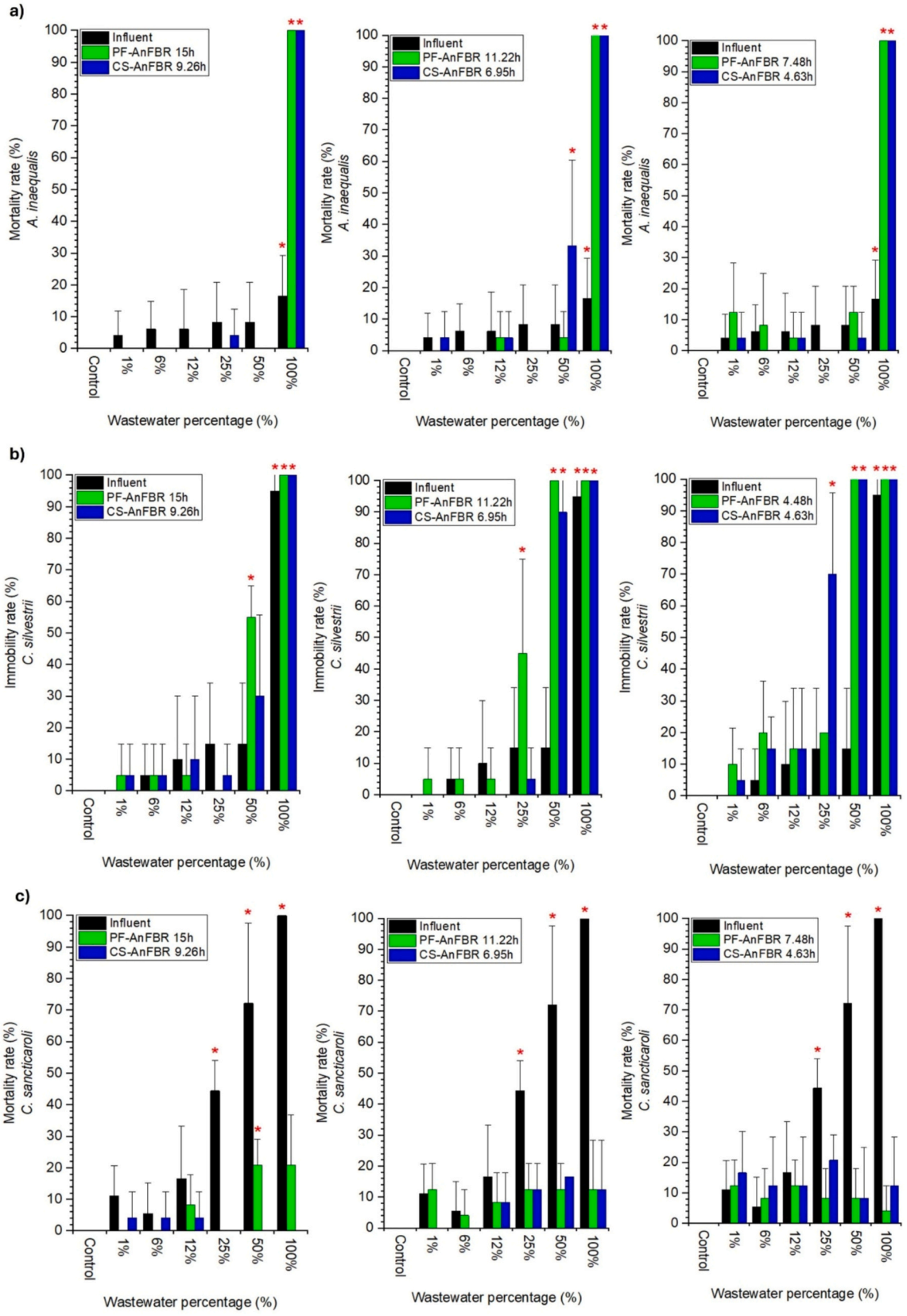

Fig. 4. Mortality and immobility rates for aquatic species after exposure to PF-AnFBR and CS-AnFBR wastewater influents and effluents across tested percentages. a) mortality rates of *A. inaequalis* in wastewater samples; b) immobility rates of *C. silvestrii* in wastewater samples; c) mortality rates of *C. sancticaroli* in wastewater samples. Note: Values expressed as average and standard deviation. *Represents treatments that showed significant differences compared to the control (multiple comparison test of *p*-values).

effluent samples from PF-AnFBR (100%) and CS-AnFBR (50% and 100%) when compared to the control samples for HRT_n of 11.22 and 7.48 h (PF-AnFBR) and 6.95 and 4.63 h (CS-AnFBR).

Statistical analysis revealed significant differences in *C. silvestrii* immobility (Fig. 4b). A substantial difference in the 15.0 h (PF-AnFBR) and 9.26 h (CS-AnFBR) HRT_n was found between 100% influent and control ($H = 61.25$; $p < 0.05$), 100% effluent from both bioreactors and control ($p < 0.05$), and 50% effluent from PF-AnFBR and control ($p < 0.05$). The 11.22 h HRT_n for PF-AnFBR revealed significant differences ($p < 0.05$) between effluent at 25, 50, and 100% and the control. The 6.95 h HRT_n for CS-AnFBR revealed significant effluent differences at 50 and 100% ($p < 0.05$). Significant differences were detected between PF-AnFBR ($p < 0.05$) and CS-AnFBR effluents ($p < 0.05$) during the lowest HRT_n (PF-AnFBR = 7.48 h, CS-AnFBR = 4.63 h).

Regarding *C. sancticaroli's* acute toxicity (Fig. 4c), the bioreactors' lab-made wastewater treatment provided positively impacted the survival of only those species, comparing influent and effluent samples from PF-AnFBR and CS-AnFBR for all the HRT_n applied. The scenario reduced species mortality to less than 21% for effluent samples. Significant statistical differences were observed for the highest HRT_n (PF-AnFBR = 15.0 h, CS-AnFBR = 9.26 h) comparing influent and effluent samples from bioreactors to the control ($H = 50.33$; $p < 0.05$): tests with 25, 50, and 100% influent and control ($p < 0.05$) and tests with 50% effluent from both bioreactors and control ($p \leq 0.05$). No significant differences were observed between the effluent samples from the bioreactors and the control for the HRT_n of 11.22 h (PF-AnFBR) and 6.95 h (CS-AnFBR) ($H = 21.82$; $p > 0.05$) and 7.48 h (PF-AnFBR) and 4.63 h (CS-AnFBR) ($H = 12.73$; $p > 0.05$).

Results in Fig. 4 indicated that treating lab-made wastewater with antibiotics in both bioreactors increased *A. inaequalis* and *C. silvestrii* acute toxicity and decreased *C. sancticaroli* acute toxicity. These different toxicological results strongly suggest that the treatment process reduces parent antibiotic concentrations and is likely to generate transformation products. The enhanced toxicity of *A. inaequalis* and *C. silvestrii* suggested that some of these derivatives may be more hazardous than the original compounds. *C. silvestrii* is sensitive to florfenicol and oxytetracycline, even at rare quantities (0.03 to 0.30 mg L^{-1}) in freshwater habitats [49]. Except for Carneiro et al. [50], antibiotic mixtures have not affected *A. inaequalis* and *C. sancticaroli* survival. In that study, residual concentrations of sulfamethoxazole and ciprofloxacin caused 100% mortality in *A. inaequalis* and 100% survival in *C. sancticaroli*.

The type of non-target species exposed strongly affects compound-toxicological interactions [51]. This could explain the lower acute effects of the treated effluent containing antibiotics on *C. sancticaroli* compared to *A. inaequalis* and *C. silvestrii*. Naturally, there is a differential sensitivity among organisms to antibiotics across different molecular classes [52]. Additive and antagonistic effects were observed of chlortetracycline, oxytetracycline, and enrofloxacin mixture in *Pseudokirchneriella subcapitata*, whereas synergistic effects were reported for mixtures in *Ankistrodesmus fusiformis*, both green algae species [53]. *P. subcapitata* showed more sensitive to tetracycline than *D. magna* under short-term exposures [54]. *Chlorella vulgaris* exhibited greater sensitivity to sulfadimethoxine compared to *D. magna* and *Daphnia similis* [55].

Isolated antibiotics at environmentally relevant concentrations (ranging from ng L^{-1} to μg L^{-1}) are unlikely to induce acute effects in aquatic invertebrates. However, considering the number of antibiotics used in combination in the present study, as well as their remaining concentrations in wastewater influents and effluents, simultaneous effects enhancing toxic outcomes such as mortality or immobilization should not be disregarded. This is important because antibiotics are toxic to bacteria and algae, which are essential for *A. inaequalis* and *C. silvestrii*'s nutritional balance and survival, and antibiotics can spread throughout the food web, affecting species interactions [56].

Chironomids demonstrate a degree of tolerance to chemical pollution, attributed to their effective antioxidant enzymatic systems, which allow for survival in stressful environments [57]. This explains the relatively low severity of treated samples for the survival of this species. The formation of potential degradation products post-treatment must also be considered. Transformation products of sulfamethoxazole and ciprofloxacin demonstrate greater toxicity to algae, daphnids, and fish compared to the parent compounds [58]. This aspect may be relevant to the findings of the current study and warrants further investigation.

3.4. Microbial community characterization

According to the Bacteria Domain taxonomy, PF-AnFBR had 161,545 16S rRNA gene sequences, CS-AnFBR had 153,415, and the inoculum had 19,364 (Fig. S3a). For PF-AnFBR, CS-AnFBR, and inoculum sequences amplicon sequence variants (ASV) 419, 364, and 95 were created, respectively. The Bacteria Domain ASV showed 78.7% similarity between PF-AnFBR and CS-AnFBR samples, and the reactor samples compared to the inoculum indicated 22.6% for PF-AnFBR and 24.0% for CS-AnFBR.

CS-AnFBR showed higher ecological diversity ($H = 4.17$; 1-D = 0.97) compared to PF-AnFBR ($H = 3.73$; 1-D = 0.90) and inoculum ($H = 3.46$; 1-D = 0.95). PF-AnFBR had higher species richness (Chao-1 = 419), followed by CS-AnFBR (Chao-1 = 364) and inoculum (Chao-1 = 95); all samples exhibited low dominances (D = 0.10) for Bacteria Domain (Table S5). The Hutcheson statistical test revealed significant differences in the samples ($p < 0.05$). The bioreactors samples exhibit high similarity, high Shannon-Wiener indices ($H > 3.50$), high Simpson indices ($0.75 < 1\text{-}D < 1.00$), and low dominance ($D < 0.50$), while the inoculum sample exhibits high Shannon-Wiener and Simpson indices ($3.00 < H < 3.50$; $0.75 < 1\text{-}D < 1.00$) and low dominance ($D < 0.50$) [59].

Proteobacteria (53.2% and 18.6%), Firmicutes (11.6% and 32.3%), Bacteroidetes (7.70% and 8.82%), Spirochaetes (4.17% and 7.45%), Chloroflexi (3.41% and 13.3%), and Desulfobacteriota (7.55% and 8.21%) were found in PF-AnFBR and CS-AnFBR, respectively, being common in anaerobic bioreactors and metabolically active [60], and acting on the co-metabolic biodegradation of aromatic compounds, such as antibiotics of this study [61,62]. *Aeromonas* (27.9%) and *Pseudomonas* (10.9%) from the Proteobacteria phylum were most prevalent in PF-AnFBR, whereas *Anaerolineaceae UCG-001* (10.5%) and *Exiguobacterium* (8.30%) from Chloroflexi and Firmicutes were most abundant in CS-AnFBR.

Aeromonas and *Pseudomonas* are facultative anaerobic bacteria—the first one has metabolic capacity for desulfonation [63], and the second one can cleave aromatic molecules and perform ω-oxidation, β-oxidation, and desulfonation using as carbon sources [64]. They also exhibit resistance and the ability to degrade certain antibiotics, especially in aquatic environments and wastewater treatment systems. Asghari et al. [65] isolated genera from the *Pseudomonas* group from untreated hospital wastewater and observed that *P. aeruginosa* strains were able to grow in concentrations of up to 64,000 μg L^{-1} of sulfamethoxazole, cefotaxime, ceftazidime, and cefixime antibiotics. Moreover, some species of *Pseudomonas* are also recognized for biodegrading sulfonamides [66]. In *Aeromonas* strains isolated from wastewater, antibiotic resistance genes (ARGs) were identified in fluoroquinolones, aminoglycosides, β-lactams, and tetracyclines [67]. Additionally, members of the Proteobacteria phylum are frequently linked to ammonification and the dissimilatory reduction of nitrate and nitrite, facilitating nitrogen attenuation via reductive processes [68]. Firmicutes and Bacteroidetes are associated with the hydrolysis and fermentation of nitrogenous organic substances, facilitating nitrogen incorporation into microbial biomass [69].

Anaerolineaceae UCG-001 performs β-oxidation [70], whereas *Exiguobacterium* produces enzymes including alkaline proteases, phosphatase, esterase, β-galactosidase, dehydrogenase, and decarboxylase for degrading complex substances [71]. The genus *Exiguobacterium*, composed of gram-positive, motile bacteria widely distributed in various environments, including extreme and contaminated locations,

has demonstrated biotechnological potential. *E.* sp. *CAP4*, isolated from the plastisphere, exhibited a high capacity to biodegrade chloramphenicol and microplastics [72]. *E. indicum* was identified among strains capable of degrading ciprofloxacin in pharmaceutical wastewater [73].

Smithella (7.70%) and *Syntrophus* (7.30%), Desulfobacteriota genera, interact syntrophically with archeal methanogens to convert propionate into methane during anaerobic biodegradation of organic matter [74,75]. *Smithella* and *Syntrophus*, indirectly enable nitrogen and phosphorus transformations by sustaining anaerobic redox conditions and enhancing carbon flow toward methanogenesis [76]. *Bacteroidetes vadinHA17* (9.90%) genus degrades proteins and amino acids in anaerobic biodegradation [77]. Fig. 5 displays the genera of bacteria with over 1.00% abundance in PF-AnFBR, CS-AnFBR, and inoculum samples.

The biomolecular analysis for the Archaea Domain generated 1917 and 8160 sequences of the 16S rRNA gene in PF-AnFBR and CS-AnFBR, respectively, and 5030 for the inoculum (Fig. S3b). The sequences were grouped into 17, 11, and 9 ASVs for PF-AnFBR, CS-AnFBR, and inoculum, respectively. The ASV of the Archaea Domain from PF-AnFBR and CS-AnFBR showed 64.3% similarity. The similarities between the reactor samples and the inoculum were 69.2% for PF-AnFBR and 60% for CS-AnFBR.

The PF-AnFBR sample had greater Shannon-Wiener diversity (H = 1.75) and Simpson (1-D = 0.71) than the CS-AnFBR sample (H = 1.08 and 1-D = 0.58), while the inoculum showed H = 1.26 and 1-D = 0.62. PF-AnFBR had a higher richness index (Chao-1 = 17) than CS-AnFBR sample (Chao-1 = 11), while the inoculum had Chao-1 = 9 for the Archaea Domain (Table S6). D = 0.29 was the dominance index of the PF-AnFBR sample, lower than CS-AnFBR sample (D = 0.42) and the inoculum (D = 0.38). All the samples showed high similarity, low Shannon diversity (1.00 < H < 2.00), moderate Simpson (0.50 < 1-D < 0.75), and low dominance (D < 0.50) [59]. Hutcheson's analysis revealed significant differences between the indices ($p < 0.05$).

Methanothrix (formerly *Methanosaeta*) [78] and *Methanobacterium* were the most frequent genera, with 48.9% and 19.5% in the PF-AnFBR reactor and 53.2% and 37.2% in the CS-AnFBR, both from the Halobacterota phylum. The genera of archaea in the inoculum are *Methanothrix* (57.1%), from the phylum Halobacterota, and *Methanolinea* (18.7%) and *Methanoregula* (10.8%), from the phylum Euryarchaeota. Fig. 6 displays methanogenomic archaea genera with over 1.00% abundance in PF-AnFBR, CS-AnFBR, and inoculum samples.

Methanothrix is an acetotrophic methanogenic archaeon characterized by a half-saturation coefficient (K_S) for that substrate that is lower than that of other acetotrophic archaea [79], and it exhibits greater sensitivity to acidity, thriving within a strict pH range of 6.6 to 7.8 [80]. *Methanothrix* uses various enzymes in acetotrophic methanogenesis, thus being the main methane producers in anaerobic biodegradation [70]. *Methanolinea*, *Methanoregula, and Methanobacterium* convert carbon dioxide (CO_2) into methane (CH_4) in the presence of hydrogen (H_2) [81]. Additionally, *Methanobacterium* is versatile for also using acetate and formate as substrates and adapts to abiotic stresses, decoding dimyo-inositol-1,1-phosphate and n-glycerol-1-phosphate [82].

Methanothrix analysis of the inoculum, PF-AnFBR, and CS-AnFBR exhibited abundances of 57.7%, 48.9%, and 53.2%, respectively, indicating anaerobic bioreactors performance, with a sharp decline

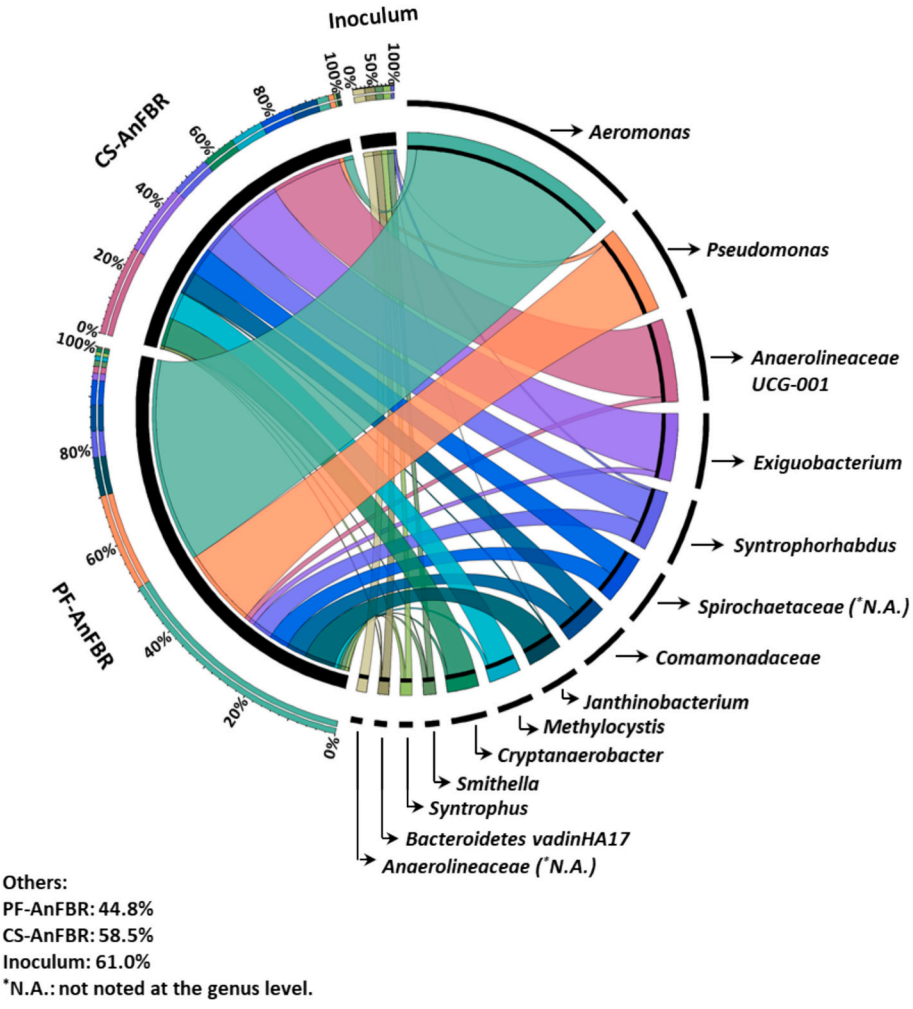

Fig. 5. Bacteria genera with highest relative abundance for the inoculum and for the samples from CS-AnFBR and PF-AnFBR applied to lab-made wastewater.

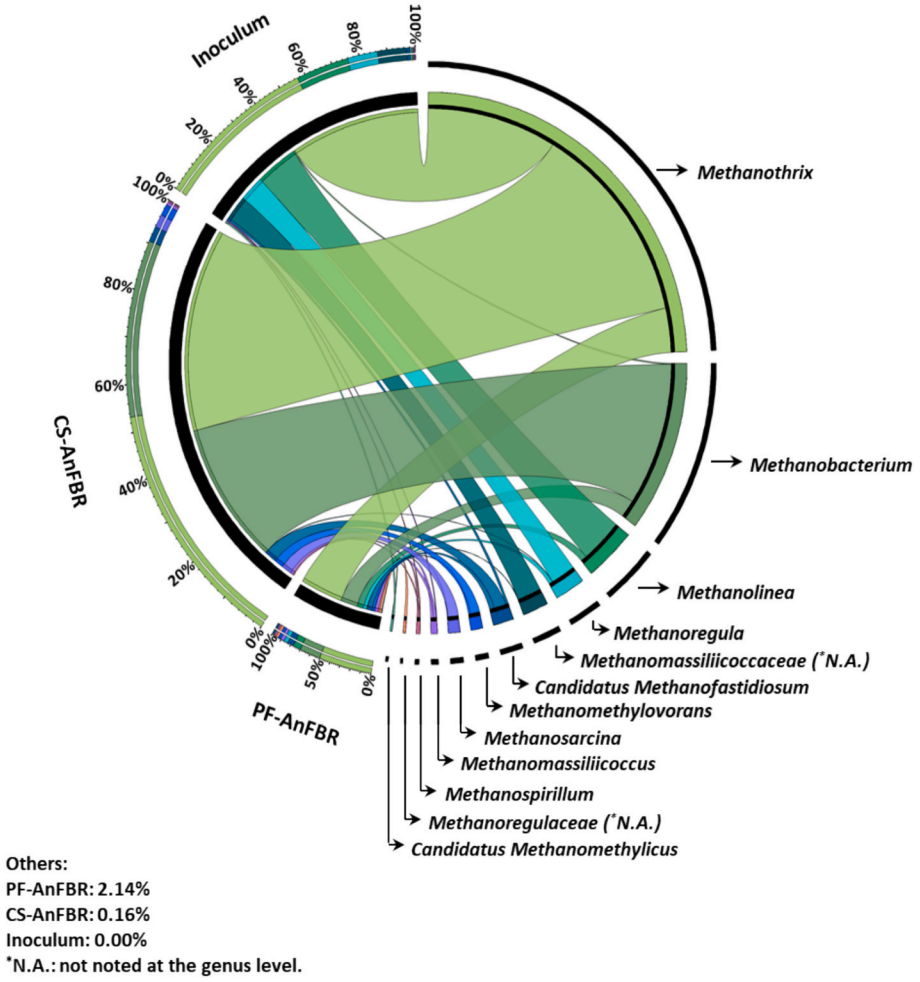

Fig. 6. Archaeal genera with highest relative abundance for the inoculum and for the samples from CS-AnFBR and PF-AnFBR applied to lab-made wastewater.

representing instability in the anaerobic digestion. Carballa et al. [83] claimed stable bioreactors in anaerobic digestion had a higher abundance of *Methanothrix* in the Archaea domain, which has been confirmed in the present study, indicating that the *Methanothrix* was the

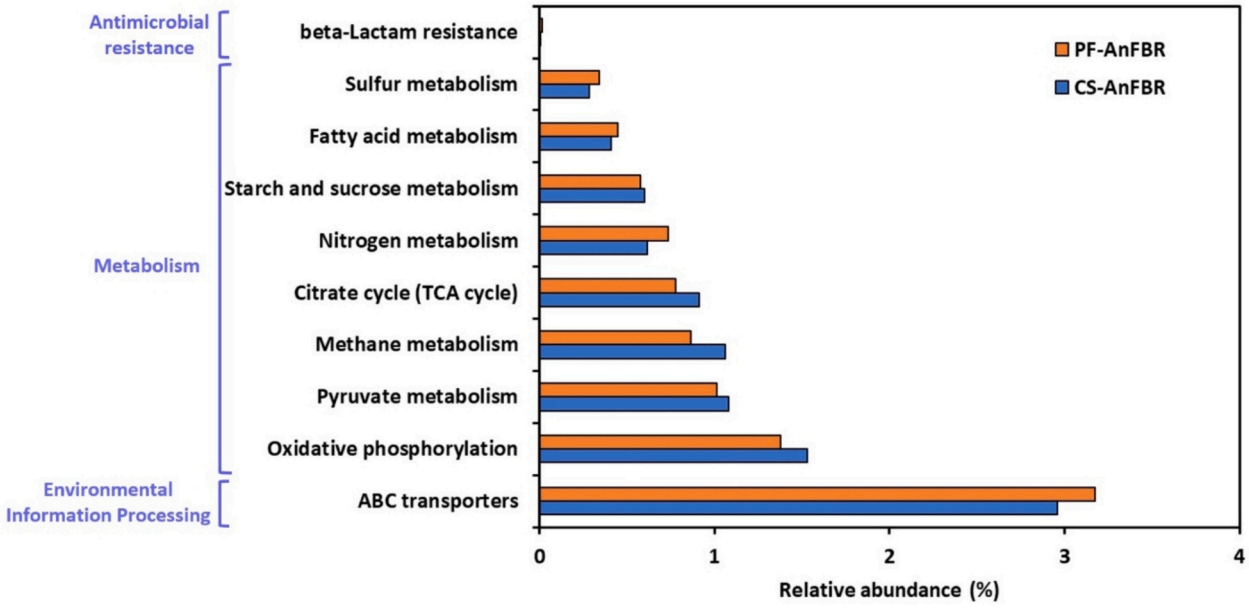

Fig. 7. The relative abundance of different microbial metabolic pathways (level 2 for KEGG) in the CS-AnFBR and PF-AnFBR applied to lab-made wastewater treatment.

most abundant in the bioreactors. Furthermore, bioreactors pH ranged from 7.18 ± 0.22 to 7.62 ± 0.31 for PF-AnFBR and from 7.30 ± 0.16 to 7.58 ± 0.28 for CS-AnFBR (Tables S7 and S8), within the ideal range (6.6 to 7.8) for *Methanothrix* growth [80]. The mesophilic conditions during PF-AnFBR and CS-AnFBR operations were crucial for the observed dominance of the *Methanothrix*, as shown in previous research [84,85].

Hydrogenotrophic methanogenic archaea, the second most abundant genera, such as *Methanobacterium*, contributed to maintaining the stability of the anaerobic reactor. In addition to the acetotrophic methanogenic archaeon *Methanothrix*, the presence of hydrogenotrophic archaea was also necessary to maintain the system's hydrogen partial pressure and stability [74]. Moreover, the efficient use of acetate and hydrogen prevents the accumulation of fermentation intermediates, hence maintaining pH levels within the optimal range for microbial growth and nutrient absorption (Tables S7–S8). The high ecological diversity (H and 1-D) and richness (Chao-1) and the low dominance (D) indices observed for the microbial community of both bioreactors brought stability to the anaerobic digestion process [86].

KEGG orthology levels (Fig. 7) identified significant metabolic pathways associated with the anaerobic biodegradation of the tested antibiotics during PF-AnFBR and CS-AnFBR operations. ABC transporters exhibited the highest proportions (PF-AnFBR = 3.17; CS-AnFBR = 2.96), followed by oxidative phosphorylation, pyruvate metabolism, methane metabolism, the citrate cycle (TCA cycle), nitrogen metabolism, starch and sucrose metabolism, fatty acid metabolism, and sulfur metabolism. The anticipated enhancement of these routes corroborates the observed biodegradation patterns, especially under plug-flow settings where prolonged and consistent biomass–substrate interaction promoted biologically mediated removal processes.

The metabolic pathway of ABC transporters is a recognized mechanism in the biodegradation of fluoroquinolones, sulfonamides, and diaminopyrimidines, in which intracellular enzymes (e.g., acetate kinase and cytochrome P450) are crucial through hydroxylation, oxidation, and reduction reactions [87]. ABC transporters play a significant role in substrate uptake, the efflux of toxic substances, and resistance mechanisms aligning with the prevalence of genera such as *Pseudomonas*, *Aeromonas*, and *Exiguobacterium*, which are recognized for possessing multiple transporter systems linked to antibiotic tolerance and co-metabolic biodegradation [74]. The oxidative phosphorylation pathway is related to the β-oxidation of aromatic compounds [88] (e.g., the 12 antibiotics of this study). Energy metabolism genes (e.g., methane metabolism, sulfur metabolism, nitrogen metabolism, oxidative phosphorylation, and the TCA cycle) contribute to the antibiotics co-metabolic biodegradation [89].

Co-metabolic biodegradation is defined as "the transformation of an organic compound by a microorganism that is unable to use the substrate as a source of energy or of one of its constituent elements" [90] and is a promising approach for microbial biodegradation of diaminopyrimidines, fluoroquinolones, and sulfonamides in the anaerobic digestion process, which involves all main functional profile inferences previously observed [61,88,91]. The initial stage of anaerobic digestion, called hydrolysis, releases hydrolytic enzymes that initiate the co-metabolic biodegradation. In the acetogenic step, bacteria from the Firmicutes phylum, which are strict anaerobes, acetogenic, and syntrophic, providing acetate, fumarate, and hydrogen for the methanogenic step [92]. The aromatic compounds biodegradation is related to the methanogenic stage, in which acetate kinase plays a fundamental role [88]. It participates in the final stage of acetogenesis in fermentative bacteria, performing the dephosphorylation of acetyl phosphate to acetate and catalyzes the transfer of ATP to acetate through the phosphorylation of acetyl phosphate to acetate [61]. It is fundamental in methane metabolism and can biodegrade smaller aromatic compounds (up to 2 rings) [91], such as the 12 antibiotics considered in the current study.

Some bacteria genera stand out regarding the performance of the microbial community in PF-AnFBR and CS-AnFBR when the 12 antibiotics are removed. The *Syntrophorhabdus* genus exhibited relative abundances of 2.85% (PF-AnFBR) and 4.82% (CS-AnFBR), establishing an obligatory syntrophic relationship with hydrogenotrophic methanogenic archaea, thereby degrading aromatic compounds. *Syntrophorhabdus* showed bamA and putative OCH CoA hydrolase genes involved in aromatic rings biodegradation [93]. Additionally, *Pseudomonas* (10.9%), involved in all stages of biodegradation and performing oxidation, desulfonation, and cleavage of aromatic compounds [64], were detected in PF-AnFBR.

Antibiotics concentration in lab-made wastewater during bioreactors operation (10.0 μg L^{-1}) did not affect their methanogenic activity negatively, and the archaea assisted in the antibiotic's biodegradation. As an example, previous studies indicated that the methanogenic activity of acetotrophic archaea (*Methanothrix* and *Methanosarcina*) directly contributes to the biodegradation of sulfonamides, and concentrations above 40.0 mg L^{-1} of sulfonamides cause the inhibition of those archaea [61,91,94]. Therefore, the operational conditions, namely, pH and antibiotic concentration, applied to PF-AnFBR and CS-AnFBR did not harm the activities of the microbial community, thus contributing to the co-metabolic biodegradation of antibiotics.

It is important to note that the functional pathways presented are derived from 16S rRNA gene data utilizing predictive bioinformatics methods (Fig. 7). This work did not conduct quantitative PCR or transcriptome validation of essential functional genes, such as CYP450 families or ABC transporter genes. Consequently, the data are to be regarded as suggestive of metabolic potential rather than definitive gene expression. Nonetheless, the robust correlation among anticipated activities, reactor performance, and the extensively documented metabolic capacities of the predominant species provide mechanistic validation for the suggested removal pathways. Future research employing qPCR or metatranscriptomic methodologies is advised to quantitatively validate the expression and control of these functional genes across varying hydrodynamic conditions.

4. Conclusions

This study demonstrated that the hydrodynamic regime strongly influenced the removal of antibiotics in AnFBR. The PF-AnFBR exhibited near-ideal hydraulic conditions, with minimal dead zones ($V_d < 2.38\%$) and short-circuiting ($Z_c \approx 1.0$), as validated by the AxD model (NRMSE <6.5%). However, the CS-AnFBR exhibited significant non-idealities, with high dead volumes (54–72%) and notable short-circuiting (Z_c = 0.19–0.61), fitting the TIS model well. The superior hydrodynamics of PF-AnFBR led to enhanced biodegradation, particularly for sulfonamides and TMP, which require longer contact with biomass. PF-AnFBR achieved high removal efficiencies for sulfonamides (47–98%), CIP (100%), PEF (82%), and TMP (100%). The CS-AnFBR perform better for certain fluoroquinolones via adsorption (ENR: 100%; NOR: 78%), likely due to increased turbulence exposing fresh adsorption sites. Both systems showed similar OFL removal.

Acute ecotoxicity assessments revealed that PF-AnFBR effluent showed lower toxicity levels on aquatic species compared to CS-AnFBR. The *C. sancticaroli* species showed improved survival rates. However, biodegradation products in the effluents increased toxicity for *A. inaequalis* and *C. silvestrii* species. Microbial analysis showed the abundance of key bacteria like *Pseudomonas* and *Aeromonas*, capable of cleavage and desulfonation aromatic rings, and *Methanothrix* archaea was crucial for system stability and antibiotics co-metabolic biodegradation. The microbial diversity and functional potential predicted (e.g., ABC transporters, oxidative phosphorylation), were maintained despite the antibiotic load.

In summary, this work highlights that reactor hydrodynamics is a key design parameter for optimizing anaerobic bioreactors for antibiotic removal. A plug-flow configuration (PF-AnFBR) is recommended to maximize biodegradation efficiency. However, future designs must also

incorporate ecotoxicological evaluations to ensure that the treatment process does not inadvertently increase the toxicological risk of the final effluent due to the formation of biodegradation products.

CRediT authorship contribution statement

Mateus Cottorello-Fonsêca: Writing – review & editing, Writing – original draft, Validation, Project administration, Methodology, Investigation, Formal analysis, Data curation, Conceptualization. **Gleyson B. Castro:** Writing – original draft, Validation, Methodology, Investigation, Formal analysis, Data curation. **Elias G.F. Rezende:** Writing – original draft, Validation, Methodology, Investigation, Formal analysis, Data curation. **Isabel K. Sakamoto:** Writing – review & editing, Investigation, Formal analysis. **Francisco R.S. Freitas:** Writing – review & editing, Formal analysis. **Rodrigo B. Carneiro:** Writing – review & editing. **Carolina A. Sabatini:** Formal analysis. **Rogers Ribeiro:** Writing – review & editing, Resources, Project administration. **Juliano J. Corbi:** Writing – review & editing, Resources, Project administration. **Marcelo Zaiat:** Writing – review & editing, Supervision, Resources, Project administration, Funding acquisition, Conceptualization.

Declaration of competing interest

The authors declare they have no known competing financial interests or personal relationships that might have appeared to influence the work reported in this paper.

Acknowledgements

The authors acknowledge the financial support from São Paulo Research Foundation (FAPESP) (grant numbers: 2020/15087-8, 2020/11042-0, 2022/12048-7, and 2019/22532-0), EU, and the State Research Agency (AEI) (grant number PCI2022-121990) in the framework of the collaborative international consortium PRESAGE financed under ERA-NET AquaticPollutants Joint Transnational Call (grant number 869178), Coordenação de Aperfeiçoamento de Pessoal de Nível Superior – Brasil (CAPES) – Finance Code 001, and Conselho Nacional de Desenvolvimento Científico e Tecnológico (CNPq) (grant number 150918/2025-9). They are also indebted to Dr. Maria A. T. Adorno and Prof. Dr. Álvaro J. Santos Neto for their technical support.

Appendix A. Supplementary data

Supplementary data to this article can be found online at https://doi.org/10.1016/j.jwpe.2026.109709.

Data availability

Data will be made available on request.

References

[1] M. Sharma, A. Yadav, K.K. Dubey, J. Tipple, D.B. Das, Decentralized systems for the treatment of antimicrobial compounds released from hospital aquatic wastes, Sci. Total Environ. 840 (2022) 156569, https://doi.org/10.1016/J.SCITOTENV.2022.156569.

[2] S. Bhatt, S. Chatterjee, Fluoroquinolone antibiotics: occurrence, mode of action, resistance, environmental detection, and remediation – a comprehensive review, Environ. Pollut. 315 (2022) 120440, https://doi.org/10.1016/J.ENVPOL.2022.120440.

[3] X. Van Doorslaer, J. Dewulf, H. Van Langenhove, K. Demeestere, Fluoroquinolone antibiotics: an emerging class of environmental micropollutants, Sci. Total Environ. 500–501 (2014) 250–269, https://doi.org/10.1016/J.SCITOTENV.2014.08.075.

[4] M.H. Cui, T. Sangeetha, L. Gao, A.J. Wang, Hydrodynamics of up-flow hybrid anaerobic digestion reactors with built-in bioelectrochemical system, J. Hazard. Mater. 382 (2020) 121046, https://doi.org/10.1016/J.JHAZMAT.2019.121046.

[5] G. Prasannamedha, P.S. Kumar, A review on contamination and removal of sulfamethoxazole from aqueous solution using cleaner techniques: present and future perspective, J. Clean. Prod. 250 (2020) 119553, https://doi.org/10.1016/J.JCLEPRO.2019.119553.

[6] S.G. Akpe, I. Ahmed, P. Puthiaraj, K. Yu, W.S. Ahn, Microporous organic polymers for efficient removal of sulfamethoxazole from aqueous solutions, Microporous Mesoporous Mater. 296 (2020) 109979, https://doi.org/10.1016/J.MICROMESO.2019.109979.

[7] N. Kraupner, S. Ebmeyer, M. Hutinel, J. Fick, C.F. Flach, D.G.J. Larsson, Selective concentrations for trimethoprim resistance in aquatic environments, Environ. Int. 144 (2020), https://doi.org/10.1016/j.envint.2020.106083.

[8] G.B. Castro, J.J. Corbi, M. Cottorello-Fonsêca, D. Correia, D. Raldúa, D. S. Alexandre, T.J. da S. Pinto, E. Prats, M. Faria, Fluoroquinolone and sulfonamide antibiotics (single and mixtures) impair the motor function of zebrafish larvae at environmentally relevant concentrations, Comparative Biochemistry and Physiology Part C: Toxicology & Pharmacology 290 (2025) 110143, https://doi.org/10.1016/J.CBPC.2025.110143.

[9] M. Antonopoulou, C. Kosma, T. Albanis, I. Konstantinou, An overview of homogeneous and heterogeneous photocatalysis applications for the removal of pharmaceutical compounds from real or synthetic hospital wastewaters under lab or pilot scale, Sci. Total Environ. 765 (2021) 144163, https://doi.org/10.1016/J.SCITOTENV.2020.144163.

[10] C.A.L. Chernicharo, J.B. van Lier, A. Noyola, T. Bressani Ribeiro, Anaerobic sewage treatment: state of the art, constraints and challenges, Rev. Environ. Sci. Biotechnol. 14 (2015) 649–679, https://doi.org/10.1007/s11157-015-9377-3.

[11] V. Stazi, M.C. Tomei, Enhancing anaerobic treatment of domestic wastewater: state of the art, innovative technologies and future perspectives, Sci. Total Environ. 635 (2018) 78–91, https://doi.org/10.1016/J.SCITOTENV.2018.04.071.

[12] R.B. Carneiro, C.M. Mukaeda, C.A. Sabatini, Á.J. Santos-Neto, M. Zaiat, Influence of organic loading rate on ciprofloxacin and sulfamethoxazole biodegradation in anaerobic fixed bed biofilm reactors, J. Environ. Manag. 273 (2020), https://doi.org/10.1016/j.jenvman.2020.111170.

[13] M. Cottorello-Fonsêca, G.B. Castro, J.J. Corbi, M. Zaiat, Anaerobic reactors for hospital wastewater treatment: a critical review of microbial communities in the antibiotic biodegradation and ecotoxicological impacts, Biodegradation 36 (2025), https://doi.org/10.1007/s10532-025-10207-4.

[14] G. Mockaitis, J.A.D. Rodrigues, E. Foresti, M. Zaiat, Toxic effects of cadmium (Cd2+) on anaerobic biomass: kinetic and metabolic implications, J. Environ. Manag. 106 (2012) 75–84, https://doi.org/10.1016/J.JENVMAN.2012.03.056.

[15] M.P. Cunha, L.T. Fuess, R.P. Rodriguez, P.N.L. Lens, M. Zaiat, Sulfidogenesis establishment under increasing metal and nutrient concentrations: an effective approach for biotreating sulfate-rich wastewaters using an innovative structured-bed reactor (AnSTBR), Bioresour. Technol. Rep. 11 (2020) 100458, https://doi.org/10.1016/J.BITEB.2020.100458.

[16] R.B. Carneiro, C.A. Sabatini, Á.J. Santos-Neto, M. Zaiat, Feasibility of anaerobic packed and structured-bed reactors for sulfamethoxazole and ciprofloxacin removal from domestic sewage, Sci. Total Environ. 678 (2019) 419–429, https://doi.org/10.1016/j.scitotenv.2019.04.437.

[17] A.J. Silva, J.S. Hirasawa, M.B. Varesche, E. Foresti, M. Zaiat, Evaluation of support materials for the immobilization of sulfate-reducing bacteria and methanogenic archaea, Anaerobe 12 (2006) 93–98, https://doi.org/10.1016/J.ANAEROBE.2005.12.003.

[18] M. Zaiat, A.K.A. Cabral, E. Foresti, Horizontal-flow anaerobic immobilized sludge reactor for wastewater treatment: conception and performance evaluation, Revista Brasileira de Engenharia – Caderno de Engenharia Química 11 (1994) 33–42.

[19] O. Levenspiel, Chemical reaction engineering, Wiley, Ind. Eng. Chem. Res. (1999) 688.

[20] M.R. Peña, D.D. Mara, G.P. Avella, Dispersion and treatment performance analysis of an UASB reactor under different hydraulic loading rates, Water Res. 40 (2006) 445–452, https://doi.org/10.1016/J.WATRES.2005.11.021.

[21] Y. Wang, M. Sanly, G. Brannock, Leslie, diagnosis of membrane bioreactor performance through residence time distribution measurements — a preliminary study, Desalination 236 (2009) 120–126, https://doi.org/10.1016/J.DESAL.2007.10.058.

[22] American Public Health Association (APHA), Standard Methods for the Examination of Water and Wastewater, in: American Water Works Association/American Public Works Association/Water Environment Federation, 21st ed., Washington, DC, USA, 2005.

[23] L.E. Ripley, W.C. Boyle, J.C. Converse, Improved alkalimetric monitoring for anaerobic digestion of high-strenght wastes, Water Pollut. Control Fed. 58 (1986) 406–411. http://www.jstor.org/stable/25042933 (accessed December 10, 2025).

[24] M.A.T. Adorno, J.S. Hirasawa, M.B.A. Varesche, Development and validation of two methods to quantify volatile acids (C2-C6) by GC/FID: headspace (automatic and manual) and liquid-liquid extraction (LLE), Am. J. Anal. Chem. (2014) 406–414, https://doi.org/10.4236/AJAC.2014.57049.

[25] P.C.F. Lima Gomes, I.N. Tomita, Á.J. Santos-Neto, M. Zaiat, Rapid determination of 12 antibiotics and caffeine in sewage and bioreactor effluent by online column-switching liquid chromatography/tandem mass spectrometry, Anal. Bioanal. Chem. 407 (2015) 8787–8801, https://doi.org/10.1007/s00216-015-9038-y.

[26] G.B. Castro, A.C. Bernegossi, F.R. Pinheiro, M.C. Felipe, J.J. Corbi, Effects of polyethylene microplastics on freshwater *Oligochaeta Allonais inaequalis* (Stephenson, 1911) under conventional and stressful exposures, Water Air Soil Pollut. 231 (2020), https://doi.org/10.1007/s11270-020-04845-y.

[27] ABNT, ABNT NBR Ecotoxicologia aquática-Toxicidade crônica-Método de Ensaio Com Ceriodaphnia Spp (Crustacea, Cladocera) Aquatic Ecotoxicology-Chronic Toxicity-Test Method with Ceriodaphnia Spp (Crustacea, Cladocera). www.abnt.org.br, 2017.

[28] J.J. Corbi, A.C. Bernegossi, L. Moura, M.C. Felipe, C.G. Issa, M.R.L. Silva, G. R. Gorni, Chironomus sancticaroli (Diptera, Chironomidae) as a sensitive test species: can we rely on its use after repeated generations, under laboratory

conditions? Bull. Environ. Contam. Toxicol. 103 (2019) 213–217, https://doi.org/10.1007/s00128-019-02644-8.
[29] USEPA (US Environmental Protection Agency), Short-Term Methods for Estimating the Chronic Toxicity of Effluents and Receiving Waters to Marine and Estuarine Organisms Third Edition, 2002.
[30] J.J. Corbi, G.R. Gorni, R.C. Correa, An evaluation of *Allonais inaequalis* Stephenson, 1911 (Oligochaeta: Naididae) as a toxicity test organism, Ecotoxicology and Environmental Contamination 10 (2015) 7–11, https://doi.org/10.5132/eec.2015.01.02.
[31] A.L. Fonseca, AVALIAÇÃO da QUALIDADE da ÁGUA Na BACIA do Rio Piracicaba /SP ATRAVÉS de Testes de TOXICIDADE Com INVERTEBRADOS, Universidade de São Paulo, 1997.
[32] OECD (ORGANIZATION FOR ECONOMY CO-OPERATION AND DEVELOPMENT), Test No. 235: Chironomus sp., Acute Immobilisation Test, 2011.
[33] R.I. Griffiths, A.S. Whiteley, A.G. O'donnell, M.J. Bailey, Rapid method for coextraction of DNA and RNA from natural environments for analysis of ribosomal DNA-and rRNA-based microbial community composition, Appl. Environ. Microbiol. 66 (2000) 5488–5491, https://doi.org/10.1128/AEM.66.12.5488-5491.2000.
[34] M. Cottorello-Fonsêca, E.G.F. Rezende, F.R.S. Freitas, R.B. Carneiro, I.K. Sakamoto, R. Ribeiro, M. Zaiat, Understanding the kinetics of antibiotic mixture biotransformation and microbial interactions in an anaerobic fixed-bed reactor for wastewater treatment, Bioprocess Biosyst. Eng. (2026), https://doi.org/10.1007/s00449-025-03281-8.
[35] Y. Yu, C. Lee, J. Kim, S. Hwang, Group-specific primer and probe sets to detect methanogenic communities using quantitative real-time polymerase chain reaction, Biotechnol. Bioeng. 89 (2005) 670–679, https://doi.org/10.1002/bit.20347.
[36] J.G. Caporaso, C.L. Lauber, W.A. Walters, D. Berg-Lyons, C.A. Lozupone, P. J. Turnbaugh, N. Fierer, R. Knight, Global patterns of 16S rRNA diversity at a depth of millions of sequences per sample, Proc. Natl. Acad. Sci. USA 108 (2011) 4516–4522, https://doi.org/10.1073/pnas.1000080107.
[37] R. Escudié, T. Conte, J.P. Steyer, J.P. Delgenès, Hydrodynamic and biokinetic models of an anaerobic fixed-bed reactor, Process Biochem. 40 (2005) 2311–2323, https://doi.org/10.1016/J.PROCBIO.2004.09.004.
[38] A.E. Rodrigues, Residence time distribution (RTD) revisited, Chem. Eng. Sci. 230 (2021) 116188, https://doi.org/10.1016/J.CES.2020.116188.
[39] D.D.W. Tsai, R. Ramaraj, P.H. Chen, A method of short-circuiting comparison, Water Resour. Manag. 26 (2012) 2689–2702, https://doi.org/10.1007/s11269-012-0040-2.
[40] S. Nachaiyasit, D.C. Stuckey, The effect of shock loads on the performance of an anaerobic baffled reactor (ABR). 2. Step and transient hydraulic shocks at constant feed strength, Water Res. 31 (1997) 2747–2754, https://doi.org/10.1016/S0043-1354(97)00134-6.
[41] G.H.D. Oliveira, A.J. Santos-Neto, M. Zaiat, Removal of the veterinary antimicrobial sulfamethazine in a horizontal-flow anaerobic immobilized biomass (HAIB) reactor subjected to step changes in the applied organic loading rate, J. Environ. Manag. 204 (2017) 674–683, https://doi.org/10.1016/j.jenvman.2017.09.048.
[42] Y. Arcand, S.R. Guiot, M. Desrochersa, C. Chavarieb, Impact of the Reactor Hydrodynamics and Organic Loading on the Size and Activity of Anaerobic Granules, 1994, https://doi.org/10.1016/0923-0467(94)87028-4.
[43] L.T. Fuess, L.S.M. Kiyuna, A.D.N. Ferraz, G.F. Persinoti, F.M. Squina, M.L. Garcia, M. Zaiat, Thermophilic two-phase anaerobic digestion using an innovative fixed-bed reactor for enhanced organic matter removal and bioenergy recovery from sugarcane vinasse, Appl. Energy 189 (2017) 480–491, https://doi.org/10.1016/J.APENERGY.2016.12.071.
[44] M. Zhou, C. Li, L. Zhao, J. Ning, X. Pan, G. Cai, G. Zhu, Synergetic effect of nano zero-valent iron and activated carbon on high-level ciprofloxacin removal in hydrolysis-acidogenesis of anaerobic digestion, Sci. Total Environ. 752 (2021), https://doi.org/10.1016/j.scitotenv.2020.142261.
[45] H. Li, H.L. Song, H. Xu, Y. Lu, S. Zhang, Y.L. Yang, X.L. Yang, Y.X. Lu, Effect of the coexposure of sulfadiazine, ciprofloxacin and zinc on the fate of antibiotic resistance genes, bacterial communities and functions in three-dimensional biofilm-electrode reactors, Bioresour. Technol. 296 (2020), https://doi.org/10.1016/j.biortech.2019.122290.
[46] K.M. Doretto, L.M. Peruchi, S. Rath, Sorption and desorption of sulfadimethoxine, sulfaquinoxaline and sulfamethazine antimicrobials in Brazilian soils, Sci. Total Environ. 476–477 (2014) 406–414, https://doi.org/10.1016/J.SCITOTENV.2014.01.024.
[47] X. Chen, W. Da Oh, Z.T. Hu, Y.M. Sun, R.D. Webster, S.Z. Li, T.T. Lim, Enhancing sulfacetamide degradation by peroxymonosulfate activation with N-doped graphene produced through delicately-controlled nitrogen functionalization via tweaking thermal annealing processes, Appl. Catal. B 225 (2018) 243–257, https://doi.org/10.1016/J.APCATB.2017.11.071.
[48] C. Chokejaroenrat, C. Sakulthaew, A. Angkaew, T. Satapanajaru, A. Poapolathep, T. Chirasatienpon, Remediating sulfadimethoxine-contaminated aquaculture wastewater using ZVI-activated persulfate in a flow-through system, Aquac. Eng. 84 (2019) 99–105, https://doi.org/10.1016/J.AQUAENG.2018.12.004.
[49] E.C. Freitas, O. Rocha, E.L.G. Espíndola, Effects of florfenicol and oxytetracycline on the tropical cladoceran Ceriodaphnia silvestrii: a mixture toxicity approach to predict the potential risks of antimicrobials for zooplankton, Ecotoxicol. Environ. Saf. 162 (2018) 663–672, https://doi.org/10.1016/j.ecoenv.2018.06.073.
[50] R.B. Carneiro, E. Pozzi, J.J. Corbi, M. Zaiat, Ecotoxicity and antimicrobial inhibition assessment of effluent from an anaerobic bioreactor applied to the removal of sulfamethoxazole and ciprofloxacin antibiotics from domestic sewage, Water Air Soil Pollut. 232 (2021), https://doi.org/10.1007/s11270-021-05097-0.
[51] M. González-Pleiter, S. Gonzalo, I. Rodea-Palomares, F. Leganés, R. Rosal, K. Boltes, E. Marco, F. Fernández-Piñas, Toxicity of five antibiotics and their mixtures towards photosynthetic aquatic organisms: implications for environmental risk assessment, Water Res. 47 (2013) 2050–2064, https://doi.org/10.1016/J.WATRES.2013.01.020.
[52] Z. Li, T. Lu, M. Li, M. Mortimer, L.H. Guo, Direct and gut microbiota-mediated toxicities of environmental antibiotics to fish and aquatic invertebrates, Chemosphere 329 (2023), https://doi.org/10.1016/j.chemosphere.2023.138692.
[53] S. Carusso, A.B. Juárez, J. Moretton, A. Magdaleno, Effects of three veterinary antibiotics and their binary mixtures on two green alga species, Chemosphere 194 (2018) 821–827, https://doi.org/10.1016/j.chemosphere.2017.12.047.
[54] B. Havelkova, D.H. Roušarová, Ecotoxicity of Selected Antibiotics for Organisms of Aquatic and Terrestrial Ecosystems. www.nel.edu, 2016.
[55] D.J. Huang, J.H. Hou, T.F. Kuo, H.T. Lai, Toxicity of the veterinary sulfonamide antibiotic sulfamonomethoxine to five aquatic organisms, Environ. Toxicol. Pharmacol. 38 (2014) 874–880, https://doi.org/10.1016/J.ETAP.2014.09.006.
[56] M.C. Danner, A. Robertson, V. Behrends, J. Reiss, Antibiotic pollution in surface fresh waters: occurrence and effects, Sci. Total Environ. 664 (2019) 793–804, https://doi.org/10.1016/J.SCITOTENV.2019.01.406.
[57] M.H. Ha, J. Choi, Effects of environmental contaminants on hemoglobin of larvae of aquatic midge, Chironomus riparius (Diptera: Chironomidae): a potential biomarker for ecotoxicity monitoring, Chemosphere 71 (2008) 1928–1936, https://doi.org/10.1016/J.CHEMOSPHERE.2008.01.018.
[58] T. Tang, M. Liu, Y. Chen, Y. Du, J. Feng, H. Feng, Influence of sulfamethoxazole on anaerobic digestion: Methanogenesis, degradation mechanism and toxicity evolution, J. Hazard. Mater. 431 (2022), https://doi.org/10.1016/j.jhazmat.2022.128540.
[59] E.P. Odum, Fundamentals of Ecology, 3rd ed., Oxford University Press, New York, 1971.
[60] C.F. Granatto, T.Z. Macedo, L.E. Gerosa, I.K. Sakamoto, E.L. Silva, M.B.A. Varesche, Scale-up evaluation of anaerobic degradation of linear alkylbenzene sulfonate from sanitary sewage in expanded granular sludge bed reactor, Int. Biodeterior. Biodegradation 138 (2019) 23–32, https://doi.org/10.1016/j.ibiod.2018.12.010.
[61] A.S. Oberoi, K.C. Surendra, D. Wu, H. Lu, J.W.C. Wong, S. Kumar Khanal, Anaerobic membrane bioreactors for pharmaceutical-laden wastewater treatment: a critical review, Bioresour. Technol. 361 (2022), https://doi.org/10.1016/j.biortech.2022.127667.
[62] Y. Su, J. Qian, J. Wang, X. Mi, Q. Huang, Y. Zhang, Q. Jiang, Q. Wang, Unraveling the mechanism of norfloxacin removal and fate of antibiotics resistance genes (ARGs) in the sulfur-mediated autotrophic denitrification via metagenomic and metatranscriptomic analyses, Sci. Total Environ. 922 (2024), https://doi.org/10.1016/j.scitotenv.2024.171328.
[63] T.P. Delforno, A.G.L. Moura, D.Y. Okada, I.K. Sakamoto, M.B.A. Varesche, Microbial diversity and the implications of sulfide levels in an anaerobic reactor used to remove an anionic surfactant from laundry wastewater, Bioresour. Technol. 192 (2015) 37–45, https://doi.org/10.1016/j.biortech.2015.05.050.
[64] T.P. Delforno, T.Z. Macedo, C. Midoux, G.V. Lacerda, O. Rué, M. Mariadassou, V. Loux, M.B.A. Varesche, T. Bouchez, A. Bize, V.M. Oliveira, Comparative metatranscriptomic analysis of anaerobic digesters treating anionic surfactant contaminated wastewater, Sci. Total Environ. 649 (2019) 482–494, https://doi.org/10.1016/j.scitotenv.2018.08.328.
[65] F.B. Asghari, M.H. Dehghani, R. Dehghanzadeh, D. Farajzadeh, K. Yaghmaeian, A. H. Mahvi, A. Rajabi, Antibiotic resistance and antibiotic-resistance genes of *Pseudomonas* spp. and *Escherichia coli* isolated from untreated hospital wastewater, Water Sci. Technol. 84 (2021) 172–181, https://doi.org/10.2166/wst.2021.207.
[66] C.W. Yang, W.C. Hsiao, B.V. Chang, Biodegradation of sulfonamide antibiotics in sludge, Chemosphere 150 (2016) 559–565, https://doi.org/10.1016/j.chemosphere.2016.02.064.
[67] R. Govender, I.D. Amoah, A.A. Adegoke, G. Singh, S. Kumari, F.M. Swalaha, F. Bux, T.A. Stenström, Identification, antibiotic resistance, and virulence profiling of Aeromonas and Pseudomonas species from wastewater and surface water, Environ. Monit. Assess. 193 (2021), https://doi.org/10.1007/s10661-021-09046-6.
[68] H. Navarrete-Euan, Z. Rodríguez-Escamilla, E. Pérez-Rueda, K. Escalante-Herrera, M.A. Martínez-Núñez, Comparing sediment microbiomes in contaminated and pristine wetlands along the coast of Yucatan, Microorganisms 9 (2021) 877, https://doi.org/10.3390/microorganisms9040877.
[69] X. Wei, Z. Qiu, E. Niyitanga, S. Gu, W. Shen, Effects of synthetic community and additives on microbial community structure and carbon and nitrogen transformation in chicken manure composting, J. Environ. Manag. 394 (2025) 127608, https://doi.org/10.1016/j.jenvman.2025.127608.
[70] T. Yamada, Y. Sekiguchi, A naerolineaceae, in: Bergey's Manual of Systematics of Archaea and Bacteria, Wiley, 2018, pp. 1–5, https://doi.org/10.1002/9781118960608.fbm00301.
[71] N. Pandey, Exiguobacterium, Beneficial Microbes in Agro-Ecology: Bacteria and Fungi, 2020, pp. 169–183, https://doi.org/10.1016/B978-0-12-823414-3.00010-1.
[72] Z. Tan, Y. Luo, X. Sun, Y. Huang, W. Sun, Biodegradation and bioaugmentation of the co-contamination of chloramphenicol and microplastics by *Exiguobacterium* sp. CAP4 isolated from a contaminated plastisphere, J. Hazard. Mater. 491 (2025), https://doi.org/10.1016/j.jhazmat.2025.137973.
[73] Q. Ali, R. Zainab, M. Badshah, W. Sarwar, S. Khan, G. Mustafa, T. Ibrahim, S. Ahmed, Prospecting the biodegradation of ciprofloxacin by Stutzerimonas stutzeri R2 and Exiguobacterium indicum strain R4 isolated from pharmaceutical

wastewater, H2Open Journal 7 (2024) 149–162, https://doi.org/10.2166/h2oj.2024.103.
[74] L. Leng, P. Yang, S. Singh, H. Zhuang, L. Xu, W.H. Chen, J. Dolfing, D. Li, Y. Zhang, H. Zeng, W. Chu, P.H. Lee, A review on the bioenergetics of anaerobic microbial metabolism close to the thermodynamic limits and its implications for digestion applications, Bioresour. Technol. 247 (2018) 1095–1106, https://doi.org/10.1016/J.BIORTECH.2017.09.103.
[75] M. Guo, S. Wei, M.X. Guo, M. Li, X. Qi, Y. Wang, X. Jia, Potential mechanisms of propionate degradation and methanogenesis in anaerobic digestion coupled with microbial electrolysis cell system: importance of biocathode, Bioresour. Technol. 400 (2024), https://doi.org/10.1016/j.biortech.2024.130695.
[76] L. Leng, P. Yang, S. Singh, H. Zhuang, L. Xu, W.-H. Chen, J. Dolfing, D. Li, Y. Zhang, H. Zeng, W. Chu, P.-H. Lee, A review on the bioenergetics of anaerobic microbial metabolism close to the thermodynamic limits and its implications for digestion applications, Bioresour. Technol. 247 (2018) 1095–1106, https://doi.org/10.1016/j.biortech.2017.09.103.
[77] C. Buenaño-Vargas, M.C. Gagliano, L.M. Paulo, A. Bartle, A. Graham, H.P.J. van Veelen, V. O'Flaherty, Acclimation of microbial communities to low and moderate salinities in anaerobic digestion, Sci. Total Environ. 906 (2024) 167470, https://doi.org/10.1016/J.SCITOTENV.2023.167470.
[78] M.C. Gagliano, P. Sampara, C.M. Plugge, H. Temmink, D. Sudmalis, R.M. Ziels, Functional insights of salinity stress-related pathways in metagenome-resolved *Methanothrix* genomes, Appl. Environ. Microbiol. 88 (2022), https://doi.org/10.1128/aem.02449-21.
[79] R.E. Speece, Anaerobic Biotechnology for Industrial Wastewaters, Archaes press, Nashville, TN, USA, 1996.
[80] G. Patel, G. Sprott, Methanosaeta 1051 concilii gen. Nov. sp. nov. ("Methanothrix 1052 concilii") and Methanosaeta thermoacetophila nom. Rev., comb. nov, Int. J. Syst. Bacteriol. 40 (1990) 79–82, https://doi.org/10.1099/00207713-40-1-79.
[81] J. Guo, Y. Peng, B.J. Ni, X. Han, L. Fan, Z. Yuan, Dissecting microbial community structure and methane-producing pathways of a full-scale anaerobic reactor digesting activated sludge from wastewater treatment by metagenomic sequencing, Microb. Cell Factories 14 (2015), https://doi.org/10.1186/s12934-015-0218-4.
[82] I. Maus, R. Stantscheff, D. Wibberg, Y. Stolze, A. Winkler, A. Pühler, H. König, A. Schlüter, Complete genome sequence of the methanogenic neotype strain Methanobacterium formicicum MFT, J. Biotechnol. 192 (2014) 40–41, https://doi.org/10.1016/J.JBIOTEC.2014.09.018.
[83] M. Carballa, L. Regueiro, J.M. Lema, Microbial management of anaerobic digestion: exploiting the microbiome-functionality nexus, Curr. Opin. Biotechnol. 33 (2015) 103–111, https://doi.org/10.1016/j.copbio.2015.01.008.
[84] K. Zhu, L. Zhang, L. Mu, J. Ma, C. Li, A. Li, Anaerobic digestion of surfactant and lipid co-existing organic waste: focusing on the antagonistic enhancement, Chem. Eng. J. 371 (2019) 96–106, https://doi.org/10.1016/J.CEJ.2019.04.033.
[85] K. Zhu, L. Zhang, X. Wang, L. Mu, C. Li, A. Li, Inhibition of norfloxacin on anaerobic digestion: focusing on the recoverability and shifted microbial communities, Sci. Total Environ. 752 (2021) 141733, https://doi.org/10.1016/J.SCITOTENV.2020.141733.
[86] Y. He, Z. Wang, C. Luo, X. Li, Z. Wang, A. Temirkhanov, Z. Nurbekova, Z. Tan, S. Zhangazin, R. Wang, Y. Chen, Deciphering the coupling of anoxic/aerobic and sulfur autotrophic denitrification: performance, antibiotic resistance genes, and microbial community structure, J. Environ. Chem. Eng. 13 (2025) 115289, https://doi.org/10.1016/J.JECE.2024.115289.
[87] X. Wang, Y. Wei, Z. Zhang, M. Cao, B. Liang, X. Yue, A. Zhou, Efficient anaerobic biodegradation of trimethoprim driven by electrogenic respiration: optimizing bioelectro-characterization, elucidating biodegradation mechanism and fate of antibiotic resistance genes systematically, J. Hazard. Mater. 492 (2025) 138070, https://doi.org/10.1016/J.JHAZMAT.2025.138070.
[88] C.F. Granatto, G.M. Grosseli, I.K. Sakamoto, P.S. Fadini, M.B.A. Varesche, Influence of cosubstrate and hydraulic retention time on the removal of drugs and hygiene products in sanitary sewage in an anaerobic expanded granular sludge bed reactor, J. Environ. Manag. 299 (2021), https://doi.org/10.1016/j.jenvman.2021.113532.
[89] R.B. Carneiro, G.M. Gomes, F.P. Camargo, M. Zaiat, Á.J. Santos-Neto, Anaerobic co-metabolic biodegradation of pharmaceuticals and personal care products driven by glycerol fermentation, Chemosphere 357 (2024), https://doi.org/10.1016/j.chemosphere.2024.142006.
[90] M. Alexander, Biodegradation and Bioremediation, Academic Press, San Diego, CA, USA, 1994.
[91] L. Gonzalez-Gil, M. Mauricio-Iglesias, D. Serrano, J.M. Lema, M. Carballa, Role of methanogenesis on the biotransformation of organic micropollutants during anaerobic digestion, Sci. Total Environ. 622–623 (2018) 459–466, https://doi.org/10.1016/j.scitotenv.2017.12.004.
[92] Q. Wen, S. Yang, Z. Chen, Mesophilic and thermophilic anaerobic digestion of swine manure with sulfamethoxazole and norfloxacin: dynamics of microbial communities and evolution of resistance genes, Front. Environ. Sci. Eng. 15 (2021), https://doi.org/10.1007/s11783-020-1342-x.
[93] Y.L. Qiu, S. Hanada, A. Ohashi, H. Harada, Y. Kamagata, Y. Sekiguchi, Syntrophorhabdus aromaticivorans gen. Nov., sp. nov., the first cultured anaerobe capable of degrading phenol to acetate in obligate syntrophic associations with a hydrogenotrophic methanogen, Appl. Environ. Microbiol. 74 (2008) 2051–2058, https://doi.org/10.1128/AEM.02378-07.
[94] Z. Cetecioglu, B. Ince, D. Orhon, O. Ince, Anaerobic sulfamethoxazole degradation is driven by homoacetogenesis coupled with hydrogenotrophic methanogenesis, Water Res. 90 (2016) 79–89, https://doi.org/10.1016/J.WATRES.2015.12.013.